

stages might be produced by cooperative activity of ER and ribosomes. These inclusion-like structures with abnormal accumulation of ER seemed likely to represent a precursor to the later neuronal LBHI observed in this line. These results imply that the deterioration of ER function and the involvement of ER might be important for formation and developing neuronal LBHI/Ast-HI in mutant SOD1 harboring FALS patients.

## DISCUSSION

Aggregated proteins or inclusions are a pathological hallmark and possible causative agent of several neurodegenerative disorders including ALS [39]. While LBHI/Ast-HI have been established as morphological hallmarks of mutant SOD1-linked FALS, little is known about the formation of these structures in neurons [6]. Several *in vitro* systems have been provided for analysis mutant SOD1 aggregation [35,36,40], however, the relationship between mutant SOD1 aggregation *in vitro* and pathological hyaline inclusions *in vivo* remains unclear. The LHI we observed in SK-N-SH cells expressing mutant SOD1 provide a direct link between *in vitro* and *in vivo* SOD1 aggregation. To our knowledge, this is the first study to show reproducible induction of LBHI/Ast-HI like structures meeting the criteria of inclusion bodies [24,26,31,38,41].

LBHIs/Ast-HIs in human FALS consist of a chaotic mixture of cytoplasmic proteins (such as SOD1, copper chaperone for SOD (CCS), peroxiredoxin 2, and glutathione peroxidase 1), cytoskeletal proteins (such as tubulin, tau protein, and phosphorylated- and nonphosphorylated neurofilament), nuclear proteins (such as neuron-specific enolase) and synaptic proteins (such as synaptophysin [24,38,41–43]). Recently, it has been published that GRP78/BiP, an ER resident chaperon protein, is also co-localized with LBHI of G93A SOD1 mice [28]. GRP78/BiP is molecular chaperone protein induced by IRE1 in response to aberrant protein folding and promotes proper protein folding. In this context, GRP78/BiP may be acting as part of the UPR response to resolve granule coated fibrils. Tobisawa et al. [35] reported increased protein levels of GRP78/BiP in motor neurons of mutant SOD1 transgenic mice, suggesting that the motor neurons in their model suffer from 'ER stress'. While the importance of ER stress or proteasome malfunction in formation of mutant SOD1 aggregates has been established [35,36,40], the mechanisms by which mutant SOD1 forms LBHI/Ast-HI in FALS remain poorly understood. In this study, we present three lines of evidence for the involvement of ER stress in early events in LBHI/Ast-HI formation. First, ER stress in neuroblastoma cells expressing mutant SOD1 results in SOD1- and ubiquitin-immunopositive LHIs, compatible with LBHI/Ast-HI, composed of granule-coated fibrils approximately 15–25 nm in diameter and granular materials (Figs. 5 and 6). Secondly, we observed similar structures in the spinal cord of L84V SOD1 transgenic mice at pre-symptomatic stages, including abnormal electron dense, i.e. stressed, ER and numerous free ribosomes. (Figs. 4 and 7). Third, positive staining against anti-KDEL antibody, which recognizes ER resident proteins such as calreticulin, GRP 94, PDI and GRP78/BiP, were observed in both the LHI and Ast-HI of L84V SOD1 transgenic mice at symptomatic stages (Fig. 6E–H). These findings support the hypothesis that ER stress induces LBHIs/Ast-HIs creation in FALS patients with mutant SOD1. Taken together, these observations suggest that LHI in neuroblastoma cells and LBHI/Ast-HI in FALS patients might develop through similar processes.

In this study, we presented evidences that ER stress causes aggregates of mutant SOD1 and formation of LHI which is compatible with LBHI/Ast-HI. However, other questions arise from these results. 1) Why did same stress induce the different

outcome of mutant SOD1 aggregation in the neuroblastoma? 2) Are the smaller aggregates competent to develop to LHIs? To answer these questions, we sought without success to identify the origin of the granule coated fibrils or SOD1 containing filamentous structure (e.g. less densely coated fibrils) in the smaller SOD1 aggregates localized to ER in L84V SOD1 expressing cells. Nevertheless, we found common features between the small aggregates in L84V SOD1 expressing SK-N-SH cells and neuronal LBHI-precursor in L84V transgenic mice, including regions of abnormal ER aggregation surrounded by abundant free ribosomes (Fig. 4B and Fig 7C). Furthermore, LHI and Ast-HI were immunopositive for the KDEL peptide present in ER-resident proteins, suggesting the involvement of ER itself in formation or development of LBHI/Ast-HI (Fig. 6E–H). We suggest that aberrant SOD1 fibril might be produced by cooperative activity of ER and ribosomes. To answer the questions, careful observation of LHI with time lapse analysis is needed.

It remains unclear why the major symptoms of ALS in patients with mutant SOD1-linked FALS do not develop until middle age, but we speculate that age-dependent changes in responses to ER stress might provide an answer. Under normal conditions, newly synthesized and misfolded proteins are refolded by chaperons such as GRP78, 94, calnexin, and calreticulin. This UPR response may be more robust in younger FALS patients and might be the reason the proteins aggregates are not observed in young patients even though mutant SOD1 is expressed. However, a decrease in protein folding or chaperone capability may occur with aging, and accumulation of misfolded proteins in the ER lumen may gradually lead to ER stress [44]. Consistent with this idea, Tobisawa et al. reported mutant SOD1 retention in the ER in COS7 cells [35] and Kikuchi et al. reported age-dependent increase of mutant SOD1 aggregation to ER in spinal cord of G93A SOD1 mice, suggesting ER dysfunction might be caused by mutant SOD1 [36]. Prolonged ER stress associated with insufficient degradation of misfolded proteins would subsequently activate apoptotic pathways. Nakagawa et al. reported that caspase-12, the ER resident caspase, is specifically cleaved and activated by ER stress, and that cells derived from mice lacking caspase-12 are resistant to ER stress [16]. In the spinal cords of G93A SOD1 mice, caspase-12 is activated in symptomatic period and can be inhibited by overexpression of XIAP (X-linked inhibitor of apoptosis protein [45,46]). Then, we analyzed activation of caspase-4 (the human orthologue of rodent caspase-12) following tunicamycin treatment. As expected, the SOD1 aggregates of the L84V SOD1-expressing neuroblastoma cells colocalized with caspase-4 (unpublished data), implying caspase-4 might contribute to cell death in our model system.

Although it can take longer than 30 years for LBHI/Ast-HI to develop in FALS patients, we could induce the formation of morphologically similar LHI within 24 hours in our simple model. Detection of the molecular targets for ER stress-induced hyaline inclusions of mutant SOD1 in our model might lead to the development of therapy that can prevent the progression of mutant SOD1-linked FALS. Ultimately, our study should contribute to the development of a simple system to analyze novel therapies for ALS.

## MATERIALS AND METHODS

### Transgenic Mice

Transgenic mice for mutant human SOD1<sup>L84V</sup> (C587BL/6 background) were created (M. Kato, et al. Transgenic mice with ALS-linked SOD1 mutant L84V. Abstract of the 31st Annual Meeting of Society for Neuroscience, San Diego, 2001). Mice were genotyped by PCR to detect the mutant SOD1 transgene using

the following primers: forward, TTGGGAGGAGGTAGT-GATTA; reverse, GCTAGCAGGATAACAGATGA. The onset of symptoms was at 5–6 months and the initial sign of the disease was usually weakness in their hindlimbs, while approximately 10% of the mice first showed weakness in their forelimbs.

### Chemicals and antibodies

We used the following antibodies: anti-SOD1 polyclonal antibody (pAb; Chemicon, Temecula, CA); anti-ubiquitin pAb and anti-KDEL mAb (Stressgen, Victoria, BC, Canada); anti-Tim17 pAb and anti-Tom20 pAb (grateful gifts by Dr. Otera and Prof. Mihara [47,48]); Alexa Fluor 488-conjugated anti-sheep IgG, Alexa Fluor 588-conjugated anti-mouse IgG antibody, and Alexa Fluor 588-conjugated anti-rabbit IgG antibody (Molecular Probes, Eugene OR); biotinylated anti-sheep IgG (Vector Laboratories, Burlingame, CA); anti-FLAG mAb (Sigma, woodlands, USA); anti-myc pAb and anti-GFP-mAb (Santa Cruz, Santa Cruz, CA); HRP-conjugated anti-sheep IgG (Jackson ImmunoResearch Laboratories Inc., West Grove, PA); and HRP-conjugated anti-mouse IgG and HRP-conjugated anti-rabbit IgG antibody (Cell Signaling Technology, Beverly, MA). Tunicamycin was obtained from Sigma.

### Cell culture and induction of ER stress

SK-N-SH human neuroblastoma cells were obtained from the Riken Cell Bank (Tsukuba, Japan), and were cultured in  $\alpha$ -MEM (Invitrogen) containing 10% fetal bovine serum at 37°C under 5% CO<sub>2</sub>. These cells were transfected with pcDNA3.1-hSOD1 and pcDNA3.1-hL84V-SOD1 to cause overexpression of wild-type or L84V mutant SOD1, respectively. G418 resistant stable neuroblastoma cell lines expressing equal levels of endogenous and exogenous SOD1 were established. In all experiments, we used cultures that were at 70–80% confluence to avoid the influence of stress induced by overgrowth. On the day of stimulation, fresh medium was added more than 1 h before exposure to stress in order to ensure the same conditions for each culture.

### Western blot analysis

SK-N-SH cells stably expressing wild-type or L84V SOD1 were washed with PBS, harvested, and lysed in TNE buffer containing 1 mM PMSF and 1% SDS. 10  $\mu$ g of protein was subjected to 12% SDS-PAGE and transferred to a PVDF membrane (Millipore Corp.). The membrane was blocked with 5% skim milk and incubated with anti-SOD1 antibody (1:1500 dilution), followed by incubation with an HRP-conjugated secondary antibody. Proteins were visualized with an ECL detection system (Amersham-Pharmacia).

### Immunocytochemistry

SK-N-SH cells stably expressing wild-type SOD1 or L84V SOD1 were treated with 1  $\mu$ g/ml of tunicamycin for 24 h. Then the cells were fixed with Zamboni's solution (0.1 M phosphate-buffered saline (PBS; pH 7.4) containing 2% paraformaldehyde (PFA) and 21% picric acid), rinsed in 0.1 M PBS, and incubated for 30 min in 0.3% H<sub>2</sub>O<sub>2</sub> to eliminate endogenous peroxidases. Next, the cells were incubated overnight at 4°C with the primary antibody (a polyclonal sheep anti-SOD1 antibody; Calbiochem) at 1:1000 in 0.1 M PBS containing 0.3% Triton X-100 and 3% bovine serum albumin (BSA). After washing in 0.1 M PBS, cells were incubated for 30 min with the secondary antibody (biotinylated anti-sheep IgG) (Vector Laboratories). After amplification with avidin-biotin complex from the ABC kit (Vector Laboratories), reaction products were visualized with 0.05 M Tris-HCl buffer (TBS; pH 7.6) containing 0.02% diaminobenzidine tetrahydrochloride

(DAB) and 0.01% hydrogen peroxide. Finally, the cells were counterstained with Mayer's hematoxylin and eosin (HE).

### Co-immunoprecipitation assay utilizing ubiquitin

Lysates of pcDNA3.1-myc-tagged ubiquitin (a kind gift from Dr. Niwa and Prof. Sobue [32])-transfected SK-N-SH cells stably expressing wild-type SOD1 or L84V SOD1 were prepared using TNE buffer (10 mM Tris-HCl, (pH 7.4), 150 mM NaCl, and 1 mM EDTA) containing 1 mM phenylmethylsulphonyl fluoride (PMSF), 2  $\mu$ g/ml aprotinin, and 1% Nonidet P-40 after treatment with or without 4  $\mu$ g/ml ALLN for 12 h. Then, 1  $\mu$ g of anti-FLAG antibody was added to 400  $\mu$ g of lysate, followed by incubation at 4°C for at least 3 h. Protein G-Sepharose (10  $\mu$ l gel) was then added and incubation was done with rotation at 4°C for 1 h. The immunoprecipitate was subjected to SDS-PAGE and transferred to a polyvinylidene fluoride (PVDF) membrane. The membrane was blocked with 5% skim milk and then was incubated with anti-Myc antibody (1:1000 dilution), followed by incubation with an HRP-conjugated secondary antibody. Proteins were visualized with an ECL detection system (Amersham-Pharmacia).

### Immunofluorescence and chemifluorescence

SK-N-SH cells expressing wild-type SOD1 or L84V SOD1 were incubated with or without tunicamycin or ALLN, rinsed in 0.02 M PBS, and fixed in Zamboni's fixative. Then the cells were incubated overnight at 4°C with an anti-SOD1 antibody (1:1000 dilution) and either anti-KDEL (1:500 dilution), anti-GM130 (1:500 dilution) or anti-ubiquitin (1:500 dilution) antibody in 0.02 M PBS containing 0.3% Triton X-100 and 3% BSA. Next, the cells were treated with fluorescent dye (Alexa Fluor 488)-conjugated donkey anti-sheep IgG (SOD1; 1:1000 dilution), fluorescent dye (Alexa Fluor 568)-conjugated goat anti-mouse IgG (KDEL, GM130; 1:1000 dilution), and goat anti-rabbit IgG (ubiquitin; 1:1000) as the secondary antibodies for 1 h at RT in 0.02 M PBS containing 3% BSA. Examination was done under a Zeiss LSM 510 microscope. For detection of SOD1 colocalization with cytochrome b5, pCMV b5-EGFP vector was transfected to the cells (kind gift from Dr. Otera and Prof. Mihara; [49]). The GFP signal was enhanced by anti-GFP antibody staining (1:100). In order to determine the localization of SOD1 in living cells, SK-N-SH cells expressing wt and L84V SOD1 were transfected with a pcDNA3.1-GFP-tagged wt and L84V SOD1 plasmid, respectively. After treatment with tunicamycin for 24 hr, the cells were further incubated with Mito-tracker or Lyso-tracker (Molecular Probes) for 30 min to visualize the mitochondria or lysosomes, respectively. Then the cells were rinsed at least three times in 0.1 M PBS and fixed with Zamboni's solution for examination under a LSM 510 confocal microscope (Zeiss, Osaka, Japan).

### Electron microscopy

SK-N-SH cells stably expressing L84V SOD1 were exposed to 1  $\mu$ g/ml tunicamycin for 24 h and then fixed at room temperature (RT) for 1 h in 0.1 M phosphate buffer (PB) containing 2.5% glutaraldehyde (GA) and 2% paraformaldehyde. Subsequently, the cells were post-fixed in 1% OsO<sub>4</sub> at RT for 1 h, dehydrated in a graded ethanol series, and embedded in epoxy resin (Quetol 812; Nisshin EM Co.). Areas containing cells with aggregates were block-mounted in epoxy resin by the direct epoxy-resin embedding method and cut into 90-nm sections. The sections were counterstained with uranyl acetate and lead citrate, and then examined using an H-7100 electron microscope (Hitachi).

## Immune Electron microscopy

As with immunocytochemistry methods above, after fixation with Zamboni solution containing 0.1% GA, the cells with anti-SOD1 antibody were developed with DAB. Then, they were post-fixed in 1% OsO<sub>4</sub> in 0.1 M PB at RT for 30 min after 1% GA in 0.1M PB re-fixation. The samples were dehydrated in a graded ethanol series and then embedded in Quetol 812. Areas containing cells with aggregate morphology were block-mounted and cut into 90-nm sections. The sections were counterstained with uranyl acetate and lead citrate, and then examined with an H-7100 electron microscope.

## Analysis of inclusion bodies (light microscopy and electron microscopy)

Sections of SK-N-SH cells containing eosinophilic hyaline inclusion bodies and spinal cord sections from transgenic SOD1 L84V mice were decolorized, rehydrated, rinsed in 0.1 M PBS, and then blocked for 1 h in 0.1 M PBS containing 0.3% Triton X-100 and 3% BSA. Next, the sections were incubated overnight at 4°C with the primary antibody (polyclonal sheep anti-SOD1 antibody at 1:500) in 0.1 M PBS containing 0.3% Triton X-100 and 3% BSA. After washing in 0.1 M PBS, sections were incubated for 30 min with the secondary antibody (biotinylated anti-sheep IgG). Subsequently, incubation was performed for 30 min in 3% H<sub>2</sub>O<sub>2</sub> to eliminate endogenous peroxidases. After amplification with avidin-biotin complex (ABC kit, Vector Laboratories), visualization of reaction products was done with 0.05 M TBS (pH 7.6) containing 1.25% DAB and 0.75% hydrogen peroxide.

For electron microscopy, samples of SK-N-SH cells expressing L84V SOD1 and spinal cords from transgenic SOD1 L84V mice were decolorized, rehydrated, and rinsed in 0.1 M PBS. The samples were further fixed and dehydrated. Then the samples were embedded directly in epoxy resin, sectioned, counterstained, and examined as described under electron microscopy section.

## SUPPORTING INFORMATION

**Figure S1** Cytosolic localization of SOD1 in wt SOD1 expressing cells under ER stress. (A-F, A'-F') Analysis of localization of SOD1 on ER. WT SOD1-expressing SK-N-SH

cells were incubated for 24 h without (A-F) or with 1 ug/ml of tunicamycin (A'-F'). Then the cells were fixed and stained using an anti-SOD1 antibody (green; A, D, A', D') and an anti-KDEL antibody (red; B, B') or an anti-GRP78 antibody (red; E, E'). GFP-cytochrome b5 were transfected to the cells and stained with anti-GFP (green; G, G') and anti-SOD1 (red; H, H') antibodies. Merged images (C, F, I, C' F', I'). (J-R, J'-R') Analysis of SOD1 localization to the mitochondria. WT SOD1-expressing SK-N-SH cells were treated as described in above. The locations of the mitochondria and SOD1 were visualized in WT SOD1-expressing SK-N-SH cells using 100 nM Mito-tracker (red; K, K'), an anti-Tim17 antibody (red; N, N') or an anti-Tom20 antibody (red; Q, Q') and an anti-SOD1 antibody (green; J, M, P, J', M', P'). Merged images (L, O, R, L', O', R'). (S-U, S'-U') Investigation of SOD1 localization to the Golgi apparatus. L84V SOD1-expressing SK-N-SH cells were treated as described in above. Then the cells were stained with anti-SOD1 antibody (green; S, S') and anti-GM130 antibody (red; T, T'). Merged images (U, U'). (V-X, V'-X') Analysis of the localization of SOD1 to the lysosomes. A GFP-tagged WT SOD1 vector was transfected into WT SOD1-expressing SK-N-SH cells. After 24 h of incubation with 1 ug/ml of tunicamycin, the cells were incubated for a further 30 min with 100 nM Lyso-tracker (red; W, W') to visualize the lysosomes. GFP channel (V, V') Merged images (X, X'). Scale bars = 20 um.

Found at: doi:10.1371/journal.pone.0001030.s001 (3.70 MB TIF)

## ACKNOWLEDGMENTS

We are grateful to Dr. Otera and Prof. Mihara (Kyusyu University, Graduate School of Medical Science) and Dr. J. Niwa and Prof. G. Sobue (Nagoya University, Graduate School of Medicine) for providing anti-Tim17 and anti-Tom20 antibodies and myc-tagged ubiquitin expression vector, respectively. We thank Dr. K. Oono, Dr. S. Matsuda and Dr. T. Kudo (Osaka University, Graduate School of Medicine) for discussion and valuable advice. We thank Dr. George Wilkinson (Max-Planck Institute of Neurobiology) for critically reading the manuscript.

## Author Contributions

Conceived and designed the experiments: SY YK TK SK MT. Performed the experiments: SY YK TK MT. Analyzed the data: SY YK TK MT JH MK MA YI SK MT. Contributed reagents/materials/analysis tools: SY YK TK MK MA YI. Wrote the paper: SY YK TK SK MT.

## REFERENCES

- Gurney ME (2000) What transgenic mice tell us about neurodegenerative disease. *Bioessays* 22: 297–304.
- Brown RH Jr., Robberecht W (2001) Amyotrophic lateral sclerosis: pathogenesis. *Semin Neurol* 21: 131–139.
- Cleveland DW, Rohstein JD (2001) From Charcot to Lou Gehrig: deciphering selective motor neuron death in ALS. *Nat Rev Neurosci* 2: 806–819.
- Rowland LP, Schneider NA (2001) Amyotrophic lateral sclerosis. *N Engl J Med* 344: 1688–1700.
- Julien JP (2001) Amyotrophic lateral sclerosis. unfolding the toxicity of the misfolded. *Cell* 104: 581–591.
- Brujin LJ, Miller TM, Cleveland DW (2004) Unraveling the mechanisms involved in motor neuron degeneration in ALS. *Annu Rev Neurosci* 27: 723–749.
- Rosen DR, Siddique T, Patterson D, Figlewicz DA, Sapp P, et al. (1993) Mutations in Cu/Zn superoxide dismutase gene are associated with familial amyotrophic lateral sclerosis. *Nature* 362: 59–62.
- Forman MS, Lee VM, Trojanowski JQ (2003) 'Unfolding' pathways in neurodegenerative disease. *Trends Neurosci* 26: 407–410.
- Kaufman RJ (2002) Orchestrating the unfolded protein response in health and disease. *J Clin Invest* 110: 1389–1398.
- Tirasophon W, Welihinda AA, Kaufman RJ (1998) A stress response pathway from the endoplasmic reticulum to the nucleus requires a novel bifunctional protein kinase/endoribonuclease (Ire1p) in mammalian cells. *Genes Dev* 12: 1812–1824.
- Wang B, Nguyen M, Breckenridge DG, Stojanovic M, Clemons PA, et al. (2003) Uncleaved BAP31 in association with A4 protein at the endoplasmic reticulum is an inhibitor of Fas-initiated release of cytochrome c from mitochondria. *J Biol Chem* 278: 14461–14468.
- Bonifacino JS, Weissman AM (1998) Ubiquitin and the control of protein fate in the secretory and endocytic pathways. *Annu Rev Cell Dev Biol* 14: 19–57.
- Travers KJ, Patil CK, Wodicka L, Lockhart DJ, Weissman JS, et al. (2000) Functional and genomic analyses reveal an essential coordination between the unfolded protein response and ER-associated degradation. *Cell* 101: 249–258.
- Urano F, Wang X, Bertolotti A, Zhang Y, Chung P, et al. (2000) Coupling of stress in the ER to activation of JNK protein kinases by transmembrane protein kinase IRE1. *Science* 287: 664–666.
- Nakagawa T, Yuan J (2000) Cross-talk between two cysteine protease families. Activation of caspase-12 by calpain in apoptosis. *J Cell Biol* 150: 887–894.
- Nakagawa T, Zhu H, Morishima N, Li E, Xu J, et al. (2000) Caspase-12 mediates endoplasmic-reticulum-specific apoptosis and cytotoxicity by amyloid-beta. *Nature* 403: 98–103.
- Katayama T, Imaizumi K, Sato N, Miyoshi K, Kudo T, et al. (1999) Presenilin-1 mutations downregulate the signaling pathway of the unfolded-protein response. *Nat Cell Biol* 1: 479–485.
- Katayama T, Imaizumi K, Honda A, Yoneda T, Kudo T, et al. (2001) Disturbed activation of endoplasmic reticulum stress transducers by familial Alzheimer's disease-linked presenilin-1 mutations. *J Biol Chem* 276: 43446–43454.

19. Dickson KM, Bergeron JJ, Shames I, Colby J, Nguyen DT, et al. (2002) Association of calnexin with mutant peripheral myelin protein-22 *ex vivo*: a basis for "gain-of-function" ER diseases. *Proc Natl Acad Sci U S A* 99: 9852–9857.
20. Nishitoh H, Matsuzawa A, Tobiume K, Saegusa K, Takeda K, et al. (2002) ASK1 is essential for endoplasmic reticulum stress-induced neuronal cell death triggered by expanded polyglutamine repeats. *Genes Dev* 16: 1345–1355.
21. Takahashi R, Imai Y (2003) Pael receptor, endoplasmic reticulum stress, and Parkinson's disease. *J Neurol* 250 Suppl 3: III25–29.
22. Takahashi R, Imai Y, Hattori N, Mizuno Y (2003) Parkin and endoplasmic reticulum stress. *Ann N Y Acad Sci* 991: 101–106.
23. Hitomi J, Katayama T, Eguchi Y, Kudo T, Taniguchi M, et al. (2004) Involvement of caspase-4 in endoplasmic reticulum stress-induced apoptosis and Abeta-induced cell death. *J Cell Biol* 165: 347–356.
24. Kato S, Takikawa M, Nakashima K, Hirano A, Cleveland DW, et al. (2000) New consensus research on neuropathological aspects of familial amyotrophic lateral sclerosis with superoxide dismutase 1 (SOD1) gene mutations: inclusions containing SOD1 in neurons and astrocytes. *Amyotroph Lateral Scler Other Motor Neuron Disord* 1: 163–184.
25. Kato S, Horiuchi S, Liu J, Cleveland DW, Shibata N, et al. (2000) Advanced glycation endproduct-modified superoxide dismutase-1 (SOD1)-positive inclusions are common to familial amyotrophic lateral sclerosis patients with SOD1 gene mutations and transgenic mice expressing human SOD1 with a G85R mutation. *Acta Neuropathol (Berl)* 100: 490–505.
26. Kato S, Saito M, Hirano A, Ohama E (1999) Recent advances in research on neuropathological aspects of familial amyotrophic lateral sclerosis with superoxide dismutase 1 gene mutations: neuronal Lewy body-like hyaline inclusions and astrocytic hyaline inclusions. *Histol Histopathol* 14: 973–989.
27. Hirano A, Kurland LT, Sayre GP (1967) Familial amyotrophic lateral sclerosis. A subgroup characterized by posterior and spinocerebellar tract involvement and hyaline inclusions in the anterior horn cells. *Arch Neurol* 16: 232–243.
28. Wate R, Ito H, Zhang JH, Ohnishi S, Nakano S, et al. (2005) Expression of an endoplasmic reticulum-resident chaperone, glucose-regulated stress protein 78, in the spinal cord of a mouse model of amyotrophic lateral sclerosis. *Acta Neuropathol (Berl)* 110: 557–562.
29. Aoki M, Abe K, Houi K, Ogasawara M, Matsubara Y, et al. (1995) Variance of age at onset in a Japanese family with amyotrophic lateral sclerosis associated with a novel Cu/Zn superoxide dismutase mutation. *Ann Neurol* 37: 676–679.
30. Shibata N, Hirano A, Kobayashi M, Siddique T, Deng HX, et al. (1996) Intense superoxide dismutase-1 immunoreactivity in intracytoplasmic hyaline inclusions of familial amyotrophic lateral sclerosis with posterior column involvement. *J Neuropathol Exp Neurol* 55: 481–490.
31. Bruijn LI, Becher MW, Lee MK, Anderson KL, Jenkins NA, et al. (1997) ALS-linked SOD1 mutant G85R mediates damage to astrocytes and promotes rapidly progressive disease with SOD1-containing inclusions. *Neuron* 18: 327–338.
32. Niwa J, Ishigaki S, Hishikawa N, Yamamoto M, Doyu M, et al. (2002) Dofrin ubiquitylates mutant SOD1 and prevents mutant SOD1-mediated neurotoxicity. *J Biol Chem* 277: 36793–36798.
33. Urushitani M, Kurisu J, Tateno M, Hatakeyama S, Nakayama K, et al. (2004) CHIP promotes proteasomal degradation of familial ALS-linked mutant SOD1 by ubiquitinating Hsp/Hsc70. *J Neurochem* 90: 231–244.
34. Higgins CM, Jung C, Ding H, Xu Z (2002) Mutant Cu, Zn superoxide dismutase that causes motoneuron degeneration is present in mitochondria in the CNS. *J Neurosci* 22: RC215.
35. Tobisawa S, Hozumi Y, Arawaka S, Koyama S, Wada M, et al. (2003) Mutant SOD1 linked to familial amyotrophic lateral sclerosis, but not wild-type SOD1, induces ER stress in COS7 cells and transgenic mice. *Biochem Biophys Res Commun* 303: 496–503.
36. Kikuchi H, Almer G, Yamashita S, Guegan C, Nagai M, et al. (2006) Spinal cord endoplasmic reticulum stress associated with a microsomal accumulation of mutant superoxide dismutase-1 in an ALS model. *Proc Natl Acad Sci U S A* 103: 6025–6030.
37. Sasaki S, Warita H, Abe K, Iwata M (2005) Impairment of axonal transport in the axon hillock and the initial segment of anterior horn neurons in transgenic mice with a G93A mutant SOD1 gene. *Acta Neuropathol (Berl)* 110: 48–56.
38. Kato S, Nakashima K, Horiuchi S, Nagai R, Cleveland DW, et al. (2001) Formation of advanced glycation end-product-modified superoxide dismutase-1 (SOD1) is one of the mechanisms responsible for inclusions common to familial amyotrophic lateral sclerosis patients with SOD1 gene mutation, and transgenic mice expressing human SOD1 gene mutation. *Neuropathology* 21: 67–81.
39. Taylor JP, Hardy J, Fischbeck KH (2002) Toxic proteins in neurodegenerative disease. *Science* 296: 1991–1995.
40. Hyun DH, Lee M, Halliwell B, Jenner P (2003) Proteasomal inhibition causes the formation of protein aggregates containing a wide range of proteins, including nitrated proteins. *J Neurochem* 86: 363–373.
41. Kato S, Horiuchi S, Nakashima K, Hirano A, Shibata N, et al. (1999) Astrocytic hyaline inclusions contain advanced glycation endproducts in familial amyotrophic lateral sclerosis with superoxide dismutase 1 gene mutation: immunohistochemical and immunoelectron microscopic analyses. *Acta Neuropathol (Berl)* 97: 260–266.
42. Kato S, Sumi-Akamaru H, Fujimura H, Sakoda S, Kato M, et al. (2001) Copper chaperone for superoxide dismutase co-aggregates with superoxide dismutase 1 (SOD1) in neuronal Lewy body-like hyaline inclusions: an immunohistochemical study on familial amyotrophic lateral sclerosis with SOD1 gene mutation. *Acta Neuropathol (Berl)* 102: 233–238.
43. Kato S, Saeki Y, Aoki M, Nagai M, Ishigaki A, et al. (2004) Histological evidence of redox system breakdown caused by superoxide dismutase 1 (SOD1) aggregation is common to SOD1-mutated motor neurons in humans and animal models. *Acta Neuropathol (Berl)* 107: 149–158.
44. Bassik MC, Scorrano L, Oakes SA, Pozzan T, Korsmeyer SJ (2004) Phosphorylation of BCL-2 regulates ER Ca(2+) homeostasis and apoptosis. *Embo J* 23: 1207–1216.
45. Wootz H, Hansson I, Korhonen L, Lindholm D (2006) XIAP decreases caspase-12 cleavage and calpain activity in spinal cord of ALS transgenic mice. *Exp Cell Res* 312: 1890–1898.
46. Wootz H, Hansson I, Korhonen L, Napankangas U, Lindholm D (2004) Caspase-12 cleavage and increased oxidative stress during motoneuron degeneration in transgenic mouse model of ALS. *Biochem Biophys Res Commun* 322: 281–286.
47. Ishihara N, Mihara K (1998) Identification of the protein import components of the rat mitochondrial inner membrane, rTIM17, rTIM23, and rTIM44. *J Biochem (Tokyo)* 123: 722–732.
48. Kanaji S, Iwahashi J, Kida Y, Sakaguchi M, Mihara K (2000) Characterization of the signal that directs Tom20 to the mitochondrial outer membrane. *J Cell Biol* 151: 277–288.
49. Kato H, Sakaki K, Mihara K (2006) Ubiquitin-proteasome-dependent degradation of mammalian ER stearoyl-CoA desaturase. *J Cell Sci* 119: 2342–2353.

ORIGINAL ARTICLE

## Intrathecal Delivery of Hepatocyte Growth Factor From Amyotrophic Lateral Sclerosis Onset Suppresses Disease Progression in Rat Amyotrophic Lateral Sclerosis Model

Aya Ishigaki, MD, PhD, Masashi Aoki, MD, PhD, Makiko Nagai, MD, PhD, Hitoshi Warita, MD, PhD, Shinsuke Kato, MD, PhD, Masako Kato, MD, PhD, Toshikazu Nakamura, PhD, Hiroshi Funakoshi, MD, PhD, and Yasuto Itoyama, MD, PhD

### Abstract

Hepatocyte growth factor (HGF) is one of the most potent survival-promoting factors for motor neurons. We showed that introduction of the HGF gene into neurons of G93A transgenic mice attenuates motor neuron degeneration and increases the lifespan of these mice. Currently, treatment regimens using recombinant protein are closer to clinical application than gene therapy. To examine its protective effect on motor neurons and therapeutic potential we administered human recombinant HGF (hrHGF) by continuous intrathecal delivery to G93A transgenic rats at doses of 40 or 200  $\mu$ g and 200  $\mu$ g at 100 days of age (the age at which pathologic changes of the spinal cord appear, but animals show no clinical weakness) and at 115 days (onset of paralysis), respectively, for 4 weeks each. Intrathecal administration of hrHGF attenuates motor neuron degeneration and prolonged the duration of the disease by 63%, even with administration from the onset of paralysis. Our results indicated the therapeutic efficacy of continuous intrathecal administration of hrHGF in transgenic rats and should lead to the consideration for further clinical trials in amyotrophic lateral sclerosis using continuous intrathecal administration of hrHGF.

**Key Words:** Amyotrophic lateral sclerosis, Continuous intrathecal delivery, Hepatocyte growth factor, Neurodegeneration, Superoxide dismutase-1 (SOD1), Transgenic rat.

From the Department of Neurology (AI, MA, MN, HW, YI), Tohoku University Graduate School of Medicine, Sendai, Japan; Tohoku University Hospital ALS Center (AI, MA, HW, YI), Sendai, Japan; Department of Neuropathology (SK), Institute of Neurological Sciences, Faculty of Medicine Tottori University, Yonago, Japan; Division of Pathology (MK), Tottori University Hospital, Yonago, Japan; and Division of Molecular Regenerative Medicine (TN, HF), Department of Biochemistry and Molecular Biology, Osaka University Graduate School of Medicine, Osaka, Japan.

Send correspondence and reprint requests to: Masashi Aoki, MD, PhD, Department of Neurology, Tohoku University Graduate School of Medicine, 1-1 Seiryō-machi, Sendai 980-8574, Japan; E-mail: aokim@mail.tains.tohoku.ac.jp

This work was supported by a grant from the Ministry of Health, Labor, and Welfare, Japan (YI, MA, SK, HF). Research funding was also provided by the Haruki ALS Research Foundation (YI, MA, HW) and by a Grant-in-Aid for Scientific Research from the Ministry of Education, Culture, Sports, Science, and Technology, Japan (MA, SK, HF).

### INTRODUCTION

Amyotrophic lateral sclerosis (ALS) is a fatal neurodegenerative disease caused by selective motor neuron death (1). Approximately 10% of cases of ALS are inherited, usually as an autosomal dominant trait (2). In ~25% of familial cases, the disease is caused by mutations in the gene encoding cytosolic copper-zinc superoxide dismutase (SOD1) (3–5). The cause of ALS is still unclear, and clinical trials have as yet failed to identify any truly effective therapeutic regimens for ALS, with only riluzole providing a modest improvement in survival. Various substances have been shown to have therapeutic effects in a murine model of ALS. However, there have been a few reports of prolongation of survival with treatment starting around the time of disease onset (6–12).

We (13) and another group (14) developed a rat model of ALS expressing a human SOD1 transgene with 2 ALS-associated mutations: glycine to alanine at position 93 (G93A) and histidine to arginine at position 46 (H46R) (3, 5). Similar to its murine counterpart, this rat transgenic (Tg) ALS model reproduces the major phenotypic features of human ALS. Some experimental manipulations are difficult in Tg mice because of size limitations; however, this Tg rat model allows routine implantation of infusion pumps for intrathecal drug delivery. Intrathecal drug application is a well-established method for therapy and has been used in clinical trials in patients with ALS (15). This route of administration bypasses the blood-brain barrier, allowing rapid access to potential binding sites for the test compound in the spinal cord (16).

Hepatocyte growth factor (HGF) was first identified as a potent mitogen for mature hepatocytes and was first cloned in 1989 (17). Detailed studies indicated that HGF is expressed in the CNS (18) and is a novel neurotrophic factor (19, 20). HGF is one of the most potent survival-promoting factors for motor neurons, comparable to glial cell line-derived neurotrophic factor *in vitro* (21). Sun et al (22) reported that introduction of the HGF gene into neurons of G93A Tg mice attenuates motor neuron degeneration and increases the lifespan of these mice. Thus, HGF is a good candidate agent for treatment of ALS. Currently, treatment using recombinant protein is closer to clinical application than gene therapy. However, HGF has a very

short half-life (23–25) and shows poor penetration into the CNS. Therefore, we examined the effects of continuous intrathecal delivery of human recombinant HGF (hrHGF) into Tg rats using implanted infusion pumps for selective and less invasive supply of HGF to the spinal cord.

## MATERIALS AND METHODS

### Animal Preparation and Clinical Evaluation

G93A Tg rats were genotyped by polymerase chain reaction (PCR) assay using DNA obtained from the tail as described (13). To examine the dose and effects of hrHGF on disease onset, we began administration of 40 or 200  $\mu$ g of hrHGF (provided by H. Funakoshi and T. Nakamura, Osaka University, Osaka, Japan) or vehicle (0.1 M sulfoxide PBS) for 4 weeks to groups of eight 100-day-old Tg rats, when the pathologic changes of the spinal cord appeared, but the animals did not show weakness. All animals were killed at 130 days by deep anesthesia, and the spinal cords were examined. Because treatment of patients with ALS patients is initiated only after diagnosis based on clinical signs and symptoms, we tested the effects of hrHGF on survival with administration beginning at around the age of onset of paralysis. We administered 200  $\mu$ g of hrHGF or vehicle alone to groups of eight 115-day-old G93A Tg rats for 4 weeks, and the animals were observed until their death. To analyze the mechanism of action of hrHGF administration beginning at onset of paralysis we treated groups of six 115-day-old G93A Tg rats with 100  $\mu$ g of hrHGF or with vehicle alone for 2 weeks (a dose comparable to 200  $\mu$ g for 4 weeks). All rats were killed 2 weeks after commencement of administration of hrHGF, and their lumbar spinal cords were examined. Further groups of 3 G93A Tg rats and 3 non-Tg rats at 70, 100, and 130 days were used to measure the levels of rat HGF and c-Met. All rats were handled according to approved animal protocols of our institution and had free access to food and water throughout the experimental period and before and after pump implantation.

The onset of ALS was scored as the first observation of abnormal gait, evidence of limb weakness, or loss of extension of the hindlimbs when picked up at the base of the tail. We defined the appearance of paralysis as disease onset, although this is not a sensitive indicator and appears later than the decrease in activity (10). However, the appearance of paralysis is a suitable marker of disease onset because it is closer to the state at which patients will be diagnosed with the disease.

Footprints were collected every 3 days by letting the rats walk on a straight path after dipping their hind paws in black ink. We measured 3 strides within the area showing regular gait and calculated the means. Footprint measurements were made for rats that began treatment at 115 days. Examiners were blinded to which group each of the rats belonged in.

### Preparation of the Osmotic Pumps and Transplant Surgery

Osmotic pumps (model number 2004 or 2002; Durect Corporation, Cupertino, CA) were incubated in sterile saline

at 37°C for 40 hours to attain a constant flow rate before use. Pumps were filled to capacity with hrHGF solution or vehicle using a filling needle. An infusion tube was made by connecting a 1-cm length of polyethylene tubing (PE 60; Becton Dickinson, Franklin Lakes, NJ) to a small caliber tube 9 cm in length (PE 10; Becton Dickinson) using an adhesive (ARON ALPHA; Konishi Co., Osaka, Japan). The end of the infusion tube was connected to the shorter end of the flow moderator, the longer end of which was inserted into the pump.

Surgery for placement of the pump and intrathecal administration was performed as follows. Tg rats were anesthetized using diethyl ether and 1% halothane in a mixture of 30% oxygen and 70% nitrous oxide. The skin over the third to fifth lumbar spinal process was incised and the paravertebral muscles were separated from the vertebral lamina with scissors. The fifth lumbar vertebra was laminectomized, and the dura mater was exposed for insertion of the infusion tube. Particular care was taken not

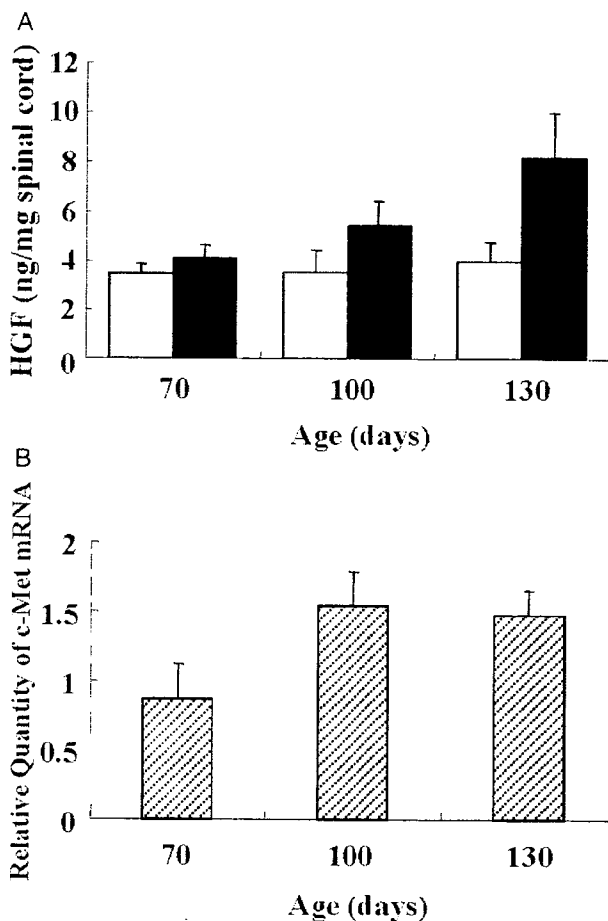


**FIGURE 1.** Increased levels of rat hepatocyte growth factor (HGF) and c-Met expression in the spinal cords of G93A transgenic (Tg) rats ( $n = 3$ ) and non-Tg rats ( $n = 3$ ). **(A)** Levels of endogenous rat HGF expression. Open bars, non-Tg rats; closed bars, G93A Tg rats. **(B)** Levels of c-Met mRNA of G93A Tg rats compared with non-Tg rats.

to injure the dura mater during laminectomy. A small hole was bored through the dura mater with a 24-gauge needle, and a polyethylene tube (PE 10, Becton Dickinson) was inserted into the subarachnoid space approximately 3 cm rostrally. A subcutaneous pocket was made into which the osmotic pump and pump side tube were implanted. The infusion tube was attached to the fascia over the paravertebral muscles at the incision margin with silk string. A drop of adhesive (ARON ALPHA) was applied, and the incision was closed by suturing the muscles and skin.

### Measurement of Rat and Human HGF in the Lumbar Spinal Cord

Slices of the fifth lumbar cord from 3 G93A Tg rats and 3 non-Tg rats at 70, 100, and 130 days as well as from 130-day-old G93A Tg rats treated with 40 or 200 µg of hrHGF or vehicle alone for 4 weeks starting at 100 days were homogenized in buffer (20 mM Tris-HCl, pH 7.5, 0.1% Tween-80, 1 mM phenylmethylsulfonyl fluoride, and 1 mM EDTA) and centrifuged at 15,000 rpm for 30 minutes. Supernatants were separated and the concentrations of rat endogenous HGF were measured using an enzyme-linked immunosorbent assay (ELISA) kit, which is specific for rat HGF without detecting human HGF (22) (Institute of Immunology, Tokyo, Japan). For measurement of human HGF in the treated rats we used a human HGF-specific ELISA kit (IMMUNIS, Institute of Immunology), which is not reactive with rat HGF (26, 27).

### Measurement of c-Met mRNA in the Lumbar Spinal Cord of Tg Rats

Aliquots of 1 µg of total RNA from the lumbar cords of rats were used as templates for synthesis of double-stranded cDNA. Real-time quantitative PCR was performed for c-Met and glyceraldehyde-3-phosphate dehydrogenase (GAPDH) [GAPDH forward primer, 5'-CCATCACTGC-CACTCAGAAGAC-3'; GAPDH reverse primer, 5'-TCA-TACTTGGCAGGTTTCTCCA-3'; GAPDH TaqMan probe, 5'(FAM)-ACCACGAGCACTGTTTCAATAGGACCC-(TAMRA)3'; c-MET forward primer, 5'-GTACGGTGTCTCCAGCATTTTT-3'; c-Met reverse primer, 5'-AGAG-

CACCACCTGCATGAAG-3'; TaqMan probe, 5'(FAM)-CGTGTTCCCTACCCCAATGTATCCGT-(TAMRA)3']. An ABI Prism 7700 Sequence Detection System (Applied Biosystems Perkin-Elmer, Foster City, CA) was used to monitor emission intensities using the above primer pairs and TaqMan fluorogenic probes. The c-Met mRNA level of G93A Tg rats relative to non-Tg rats was calculated using the Comparative C<sub>T</sub> Method (Applied Biosystems).

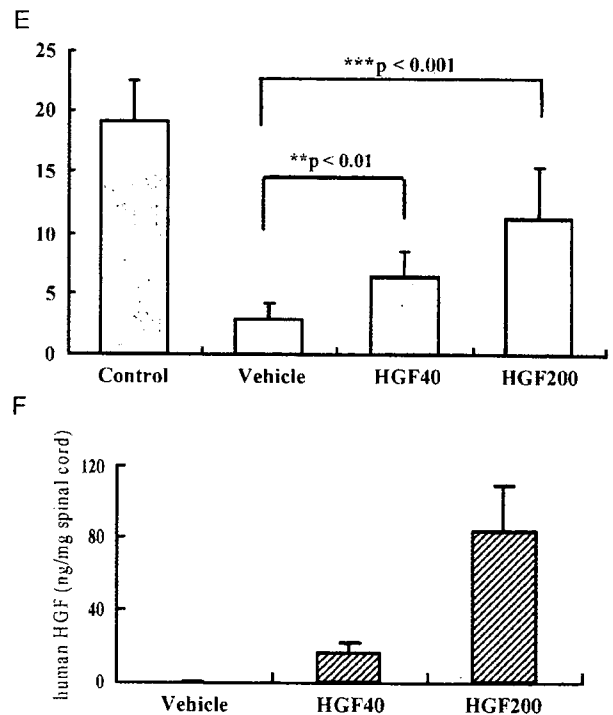
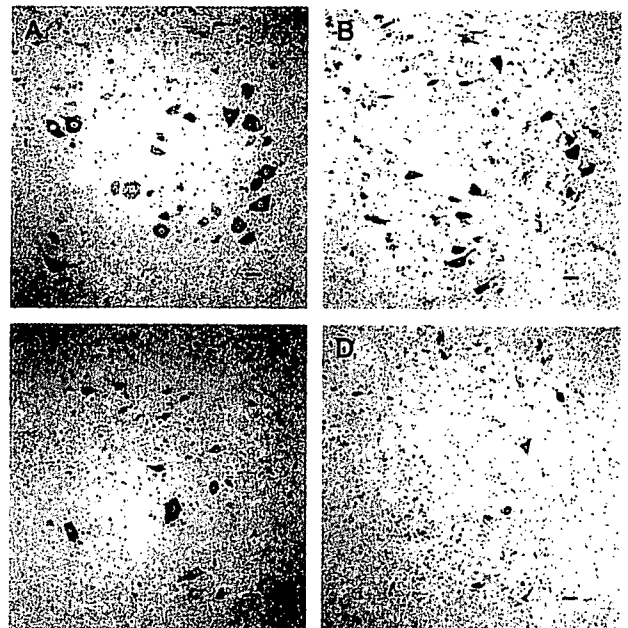


**FIGURE 2.** Intrathecal administration of hepatocyte growth factor (HGF) to G93A transgenic (Tg) rats at 100 days showed a protective effect against motor neuron death. **(A–D)** Histologic evaluation of the anterior horn with Nissl staining at 130 days: **(A)** lumbar cord of non-Tg rats; **(B)** 200 µg of human recombinant HGF (hrHGF)-treated; **(C)** 40 µg of hrHGF-treated; and **(D)** vehicle-treated G93A Tg rats. Scale bar = 40 µm. **(E)** Quantitative morphometric evaluation of surviving motor neurons of the fifth lumbar anterior horn at 130 days. We counted neurons that were >40 µm in diameter. Significantly larger numbers of motor neurons survived in hrHGF-treated G93A Tg rats ( $p < 0.01$  and  $p < 0.001$ , 40 and 200 µg of hrHGF, respectively), compared with vehicle-treated G93A Tg rats ( $n = 8$  in each group). **(F)** Levels of human HGF concentration in lumbar spinal cords of G93A Tg rats treated with 200 µg of hrHGF, 40 µg of hrHGF, and vehicle.

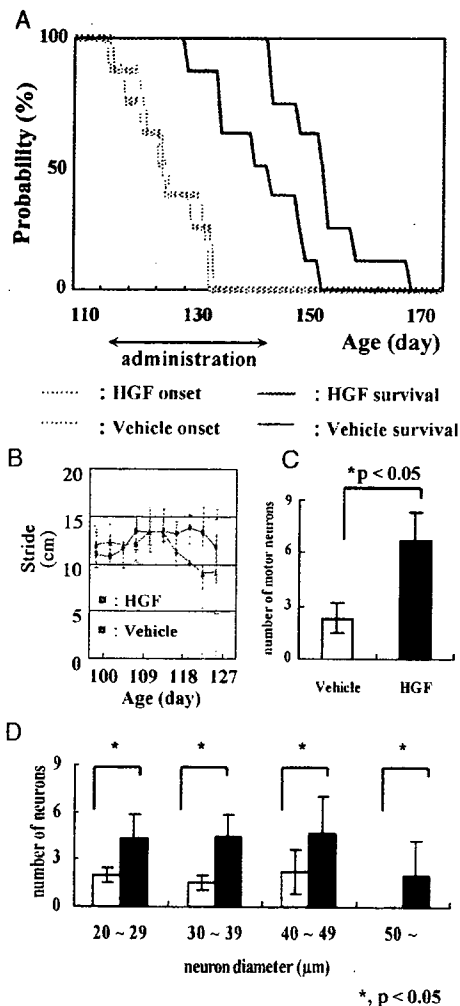


**FIGURE 3.** Intrathecal administration of hepatocyte growth factor (HGF) from 115 days (just before disease onset) retarded disease progression. **(A)** Survival periods were  $143.25 \pm 17.0$  days in the vehicle-treated group (solid blue line) and  $154.3 \pm 16.4$  days in the  $200 \mu\text{g}$  of human recombinant HGF (hrHGF)-treated group (solid red line). Survival of hrHGF-treated animals was extended significantly ( $p = 0.0135$ ), although there were no significant differences in onset (dotted lines,  $n = 8$  in each group,  $p = 0.6346$ ). **(B)** Footprint analysis demonstrated a delay in decline of stride length in G93A transgenic (Tg) rats treated with  $200 \mu\text{g}$  of hrHGF relative to vehicle-treated G93A Tg rats (error bars,  $\pm$  SD). **(C, D)** Quantitative morphometric evaluation of surviving motor neurons that were  $>40 \mu\text{m}$  in diameter **(C)** and neuron size distribution **(D)** in the fifth lumbar anterior horn of G93A Tg rats 2 weeks after administration from 115 days. Significantly larger number of motor neurons survived in the hrHGF-treated G93A Tg rats compared with vehicle-treated G93A Tg rats ( $6.7 \pm 1.6$  vs  $2.3 \pm 0.9$ ;  $p = 0.002$ ,  $n = 6$  in each group) **(C)**.

## Histopathologic and Immunohistochemical Analyses

To examine the dose and effects of hrHGF against disease onset, we began administration of 40 or  $200 \mu\text{g}$  of hrHGF or vehicle alone to groups of eight 100-day-old Tg rats each for 4 weeks. At 130 days, G93A Tg rats were administered hrHGF or vehicle, and non-Tg rats were deeply anesthetized with diethyl ether and killed for histopathologic evaluation. To examine the effects of hrHGF administration beginning at onset of paralysis,  $100 \mu\text{g}$  of HGF or vehicle alone was administered to groups of six 115-day-old Tg rats for 2 weeks. These animals were killed by deep anesthesia with diethyl ether 2 weeks after the operation. Under deep anesthesia these animals were perfused via the aorta with physiologic saline at  $37^\circ\text{C}$  and their lumbar spinal cords were removed. The fifth lumbar spinal cord tissue was embedded in OCT compound (Sakura Finetek Japan Co., Tokyo, Japan), frozen in an acetone/dry ice bath after fixation with 4% paraformaldehyde, and supplemented with 0.1 M cacodylate buffer (pH 7.3) containing 30% sucrose. Other spinal cord tissue specimens were frozen in dry ice and cut into frozen sections ( $12\text{-}\mu\text{m}$ -thick) and then washed with PBS. To evaluate the effects of HGF on motor neuron loss we compared the numbers of lumbar motor neurons in each group by counting as mentioned below. To evaluate the effects of HGF on apoptosis and to determine whether HGF receptors were activated, we compared the results of immunohistochemical staining of the lumbar cords for activated caspase-3, activated caspase-9 (Cell Signaling Technology, Inc., Beverly, MA), and phosphorylated c-Met (activated HGF receptor) (BioSource International, Camerillo, CA). The staining specificity of the antibodies was assessed by preabsorption of the primary antibody with excess peptide, omission of the primary antibody, or replacement of the primary antibody with normal rabbit IgG (22). We examined every seventh section from 42 serial sections of the fifth lumbar spinal cord. We counted neurons that had a clear nucleolus and were multipolar with neuronal morphology (13, 22),  $>40 \mu\text{m}$  in diameter, and located in a defined area of the anterior horn of the spinal cord. Cell counts were performed using ImageJ software (National Institutes of Health, Bethesda, MD) on images captured electronically (28).

## Western Blotting

Lysates from the lumbar spinal cord of each rat were prepared in RIPA buffer (150 mM NaCl, 1% Nonidet P-40, 0.5% deoxycholate, 0.1% sodium dodecyl sulfate, and 50 mM Tris, pH 8.0). Equal amounts of proteins from the lysates ( $50 \mu\text{g}$ ) were resolved by sodium dodecyl sulfate-polyacrylamide gel electrophoresis, transferred onto polyvinylidene difluoride membranes, and immunoblotted. The primary antibodies used were anti-caspase-3 (Sigma-Aldrich, St. Louis, MO), anti-caspase-9 (Stressgen Biotechnologies Corporation, Victoria, BC, Canada), anti-X-linked inhibitor of apoptosis protein (XIAP) (Cell Signaling Technology, Inc.), and anti-excitatory amino acid transporter 2 (EAAT2) antibodies (Chemicon International, Temecula, CA). After incubation of membranes with HRP-coupled



secondary antibodies, proteins were visualized using ECL or ECL Plus Western Blotting Detection Reagents (Amersham Biosciences Inc., Piscataway, NJ) and a Fluorochem image analyzer (LAS-3000 mini; Fuji Photo Film Co., Tokyo, Japan).

**Statistical Analysis**

The Kaplan-Meier and log-rank test were used for statistical analyses of differences in onset and survival between groups. For statistical analyses of differences in body weight, footprint, motor neuron cell count, and Western blotting we used analysis of variance and post hoc tests. The data are reported as means ± SD.

**RESULTS**

**Measurement of the Levels of Rat HGF and c-Met Expression in Untreated Animals**

Groups of 3 G93A Tg rats and non-Tg rats at 70, 100, and 130 days were used to measure the levels of rat HGF without any treatment. In the lumbar cords of untreated G93A Tg rats, the HGF concentrations increased with disease progression (Fig. 1A). At 70 days the level of rat HGF in the lumbar cords of G93A Tg rats was  $4.05 \pm 0.6$  ng/mg and was the same as that of non-Tg rats. Increases of 35% and 107% were observed in the rat HGF level at 100 and 130 days, respectively, compared with non-Tg rats.

In addition, we measured the levels of c-Met mRNA in the lumbar spinal cords of Tg rats relative to non-Tg rats by real-time quantitative PCR. In the lumbar cords of G93A Tg rats the level of c-Met mRNA expression was the same as that in non-Tg rats at 70 days. However, a 55% increase in the level of c-Met mRNA expression compared with that of non-Tg rats was observed at 100 days and the higher level of expression was retained at 130 days (Fig. 1B).

**Administration of hrHGF to 100-Day-Old G93A Tg Rats for 4 Weeks**

To examine the efficacy of hrHGF on motor neurons in the spinal cords of Tg rats against onset of disease we administered 40 and 200 µg of hrHGF or vehicle alone to 100-day-old G93A Tg rats for 4 weeks (n = 8 in each group).

Animals were killed at 130 days, and their lumbar spinal cords were examined. Because administration of hrHGF for more than 30 days may induce antibodies against hrHGF, we did not treat rats for longer than this period. We confirmed elevation of human HGF concentrations in the lumbar cords of hrHGF-treated rats using a specific sandwich immunoassay. The mean human HGF concentrations were  $83.9 \pm 25.1$ ,  $15.6 \pm 5.4$ , and 0 ng/mg for rats treated with 200 µg of hrHGF, 40 µg of hrHGF, and vehicle, respectively (Fig. 2F). The endogenous rat HGF concentration is 4 to 5 ng/mg at this age (Fig. 1A). The human HGF concentration in the spinal cord of G93A Tg rats treated with 200 µg of hrHGF

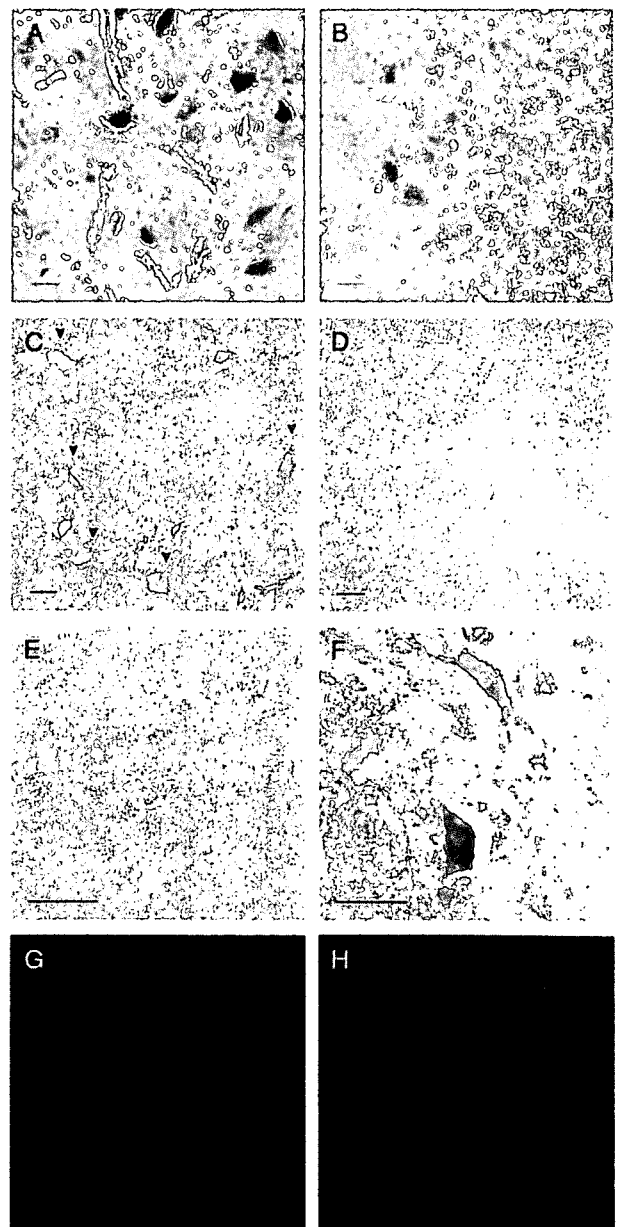


**FIGURE 4.** Sections of the fifth lumbar anterior horn from G93A transgenic (Tg) rats treated with human recombinant hepatocyte growth factor (hrHGF) (A, C, E, G) or vehicle (B, D, F, H) for 2 weeks starting at 115 days were stained with hematoxylin and eosin (A, B) and antibodies to phosphorylated c-Met (C, D), activated caspase-3 (E, F), and activated caspase-9 (G, H). Scale bar = 50 µm. There were larger numbers of remaining large motor neurons in hrHGF-treated G93A Tg rats ( $6.7 \pm 1.6$ ) (A) than in vehicle-treated G93A Tg rats ( $2.3 \pm 0.9$ ) (B). Phosphorylated c-Met staining was more distinct in hrHGF-treated G93A Tg rats (C) than in vehicle-treated G93A Tg rats (D). In contrast, activated caspase-3 staining was stronger in vehicle-treated G93A Tg rats (F) than in hrHGF-treated G93A Tg rats (E). Activated caspase-9 staining was detectable in vehicle-treated G93A Tg rats (H) compared with little reactivity in hrHGF-treated G93A Tg rats (G).

was increased by approximately 20-fold relative to the endogenous rat HGF. All vehicle-treated G93A Tg rats developed weakness in the hindlimbs with a mean onset of  $118.8 \pm 4.3$  days. Seven of 8 G93A Tg rats treated with 40  $\mu\text{g}$  of rhHGF developed the disease before 130 days. In contrast, only 3 of 8 animals treated with 200  $\mu\text{g}$  of rhHGF developed paralysis before this stage. At 130 days the average numbers of motor neurons in the ventral horn were as follows: non-Tg rats,  $19.2 \pm 3.3$ ; vehicle only,  $2.9 \pm 1.3$ ; 40  $\mu\text{g}$  of hrHGF,  $6.3 \pm 2.1$ ; and 200  $\mu\text{g}$  of hrHGF,  $11.2 \pm 4.2$ . Significantly more motor neurons survived in hrHGF-treated (40  $\mu\text{g}$ ,  $p < 0.01$ ; 200  $\mu\text{g}$ ,  $p < 0.001$ ) than in vehicle-treated G93A Tg rats (Fig. 2A–E). hrHGF prevented motor neuron death in G93A Tg rats in a dose-dependent manner.

### Administration of hrHGF to 115-Day-Old G93A Tg Rats for 4 Weeks

We next examined the therapeutic potential of HGF when administration was started at around the age of onset of paralysis. We administered 200  $\mu\text{g}$  of hrHGF or vehicle alone to 115-day-old G93A Tg rats for 4 weeks. There were no statistically significant differences ( $p = 0.6346$ ) in onset between the groups (200  $\mu\text{g}$  of hrHGF,  $126.8 \pm 13.1$  days; vehicle,  $126.3 \pm 13.8$  days) (Fig. 3A, dotted lines). In contrast, 200  $\mu\text{g}$  of hrHGF extended mean survival by 11 days compared with vehicle-treated G93A Tg rats ( $p = 0.0135$ ) (Fig. 3A, solid lines), although G93A Tg rats showed very rapid disease progression and died within 20 days of disease onset. The average periods from the onset to death were  $16.9 \pm 8.17$  and  $27.5 \pm 11.1$  days in vehicle ( $n = 8$ ) and hrHGF ( $n = 8$ ) groups, respectively. The latter represented an increase of 62.7% relative to vehicle-treated controls. Footprint analysis of stride length in 200  $\mu\text{g}$  of hrHGF-treated G93A Tg rats showed significant improvement compared with vehicle-treated G93A Tg rats at 118 days ( $p = 0.0424$ ) (Fig. 3B). Thus, despite the very rapid disease progression in this model and short treatment period of 4 weeks, hrHGF treatment improved motor performance and prolonged survival even with treatment beginning around the onset of paralysis.

Histologic evaluation of the lumbar spinal cord indicated that hrHGF treatment prevented the pathologic changes typical of Tg rats. Two weeks after commencement of administration at 129 days, vehicle-treated rats showed substantial loss of motor neurons ( $2.3 \pm 0.9$ ) compared with hrHGF-treated rats ( $6.6 \pm 1.6$ ) (Figs. 3C, 4A, B). A significantly larger number of motor neurons survived in hrHGF-treated G93A Tg rats than in vehicle-treated G93A Tg rats ( $p = 0.002$ ). Histologic evaluation of the lumbar spinal cord revealed much greater numbers of phosphorylated c-Met-positive cells (which were presumed to be motor neurons because of their large size, multipolar form, and localization in the anterior horn of the spinal cord) in hrHGF-treated G93A Tg rats compared with vehicle-treated G93A Tg rats at 2 weeks after the start of administration at 129 days (Fig. 4C, D). These observations indicated that the administered hrHGF was used in the spinal cord in G93A Tg rats. Consistent with the observation that apoptosis is involved in the pathogenesis of ALS (29–32), immunohistochemical

analyses indicated large numbers of cells positive for activated caspase-3 and caspase-9 in vehicle-treated rats (Fig. 4F, H), compared with little or no reactivity in hrHGF-treated rats (Fig. 4E, G). To assess the mechanisms of suppression of caspase-3 and caspase-9 activation in hrHGF-treated rats, we next examined the level of XIAP by Western blotting, as XIAP inhibits activation of these pro-caspases and its levels are decreased in ALS mice (31). Western blotting analysis revealed increased XIAP expression

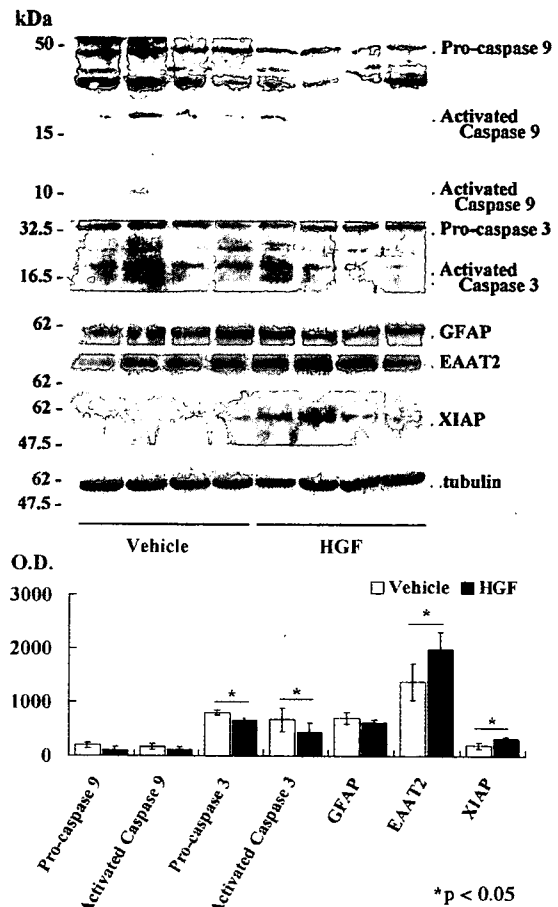


**FIGURE 5.** Caspase-3 and -9, glial fibrillary acidic protein (GFAP), excitatory amino acid transporter 2 (EAAT2), X-linked inhibitor of apoptosis protein (XIAP), and  $\beta$ -tubulin expression in the lumbar spinal cord. Western blotting of lumbar spinal cord lysates from G93A transgenic (Tg) rats treated with 100  $\mu\text{g}$  of human recombinant hepatocyte growth factor (hrHGF) or vehicle for 2 weeks from 115 days. Western blotting analysis revealed increased levels of EAAT2 and XIAP expression in the spinal cords of hrHGF-treated G93A Tg rats compared with vehicle-treated G93A Tg rats (XIAP,  $p = 0.0099$ ; EAAT2,  $p = 0.0417$ ;  $n = 4$ ). On the other hand, activated caspase-3 and -9 expression levels were decreased in hrHGF-treated G93A Tg rats. There were significant differences in caspase-3 expression between hrHGF- and vehicle-treated G93A Tg rats (pro-caspase-3,  $p = 0.0031$ ; activated caspase-3,  $0.0154$ ;  $n = 4$ ). GFAP expression was equivalent in both groups.

in the spinal cord of G93A Tg rats, and the increase in hrHGF-treated rats was only 60% of that in vehicle-treated G93A Tg rats. On the other hand, activated caspase-3 and 9 levels were decreased in hrHGF-treated G93A Tg rats ( $p = 0.0154$  and  $p = 0.2364$ , 75% and 69% of vehicle-treated G93A Tg rats, respectively). These were all considered to be effects of HGF on motor neurons. Finally, we examined whether HGF improves the function of other cell types, such as astrocytes. There was a 60% increase in glial-specific glutamate transporter (EAAT2) in hrHGF-treated rats compared with vehicle-treated controls, although there was little difference in GFAP expression levels between the 2 groups (Fig. 5).

## DISCUSSION

In this study, we demonstrated dose-dependent effects of hrHGF on motor neurons in the G93A Tg rat model of ALS, with administration starting at 100 days. Furthermore, we showed that hrHGF retards disease progression in this animal model treated from 115 days at the time of disease onset. There have been many studies of possible treatments in a mouse model of ALS (33, 34), but few agents have been shown to prolong survival with administration starting around disease onset (6–12). In this study, recombinant hrHGF retarded disease development even with administration beginning around the age onset of paralysis. Here, we showed the therapeutic effects of intrathecal delivery of a neurotrophic factor as a protein, rather than a transgene, on ALS beginning at the onset of paralysis. The average survival period of hrHGF-treated rats was 62.7% longer than that of vehicle-treated controls, comparable with the improved survival obtained by viral delivery of insulin-like growth factor-1 (6). We defined the appearance of paralysis as disease onset, although this is not a sensitive indicator and appears later than the decrease in activity (10). However, the appearance of paralysis is a clinically relevant marker of disease onset because it is closer to the state at which patients will be diagnosed with the disease.

We confirmed elevation of the human HGF concentration in the lumbar cords of hrHGF-treated G93A Tg rats using a specific sandwich immunoassay. Histologic evaluation of the lumbar spinal cord revealed greater numbers of phosphorylated c-Met-positive motor neurons in hrHGF-treated G93A Tg rats. This finding suggested that HGF receptors of motor neurons were activated well by administered hrHGF (35). These observations indicated that the administered hrHGF penetrated into the spinal cord and was utilized in the motor neurons of spinal cord. Previous studies demonstrated that many trophic factors have protective effects on motor neurons. In human trials of neurotrophic factors, such as brain-derived neurotrophic factors, glial cell line-derived neurotrophic factor, and insulin-like growth factor-1, the delivery (accessibility) of the protein to the motor neurons and glia in the spinal cord has been argued to be essential. Our results confirmed that chronic intrathecal administration with implanted infusion pumps supplied appropriate therapeutic doses to spinal cord motor neurons.

The HGF concentrations in cerebrospinal fluid are increased in many neurologic disorders, including ALS (26). In G93A Tg rats, the level of endogenous HGF in the spinal

cord showed significantly greater elevation when the pathologic changes began in the spinal cord and increased with progression of the disease compared with the level of endogenous HGF in the spinal cord of non-Tg rats. After onset, the level of endogenous HGF almost doubled relative to that in non-Tg rats (Fig. 1A). These results were compatible to observations in patients with sporadic as well as familial ALS (36, 37). The level of c-met RNA expression in the lumbar cord of G93A rats increased to 155% of the normal level from before onset, and this elevated expression was retained after onset of disease (Fig. 1B). Kato et al (36) demonstrated that autocrine and paracrine trophic support of the HGF-c-met system contributes to attenuation of the degeneration of residual spinal cord motor neurons in ALS, whereas disruption of the HGF-c-met system at an advanced stage of disease accelerates cellular degeneration (37). Administration of hrHGF delayed the pathologic changes in G93A Tg rats. This effect of HGF may be due to replenishment of the relative insufficiency of HGF in G93A Tg rats in the present study.

Consistent with the findings that apoptosis is involved in ALS (29–31), large numbers of cells immunopositive for activated caspase-3 and -9 were observed in vehicle-treated animals in contrast to little or no reactivity in hrHGF-treated rats. This result was verified by quantitative Western blotting analysis, which indicated that HGF could block caspase activation of apoptosis. Caspase-3 and -9 are the main factors involved in execution of the caspase cascade. The survival-prolonging effect of HGF may be explained by suppression of induction and activation of caspase-9, as this enzyme is involved in determining disease duration (31). These observations suggest that the mechanism of the therapeutic effect of HGF in G93A Tg rats includes inhibition of the caspase cascade or of the cell death mechanism preceding the caspase cascade. In addition, EAAT2 and XIAP expression levels were increased in the hrHGF-treated group compared with vehicle-treated controls, indicating that HGF affected not only motor neurons via inhibition of the caspase cascade but also other cell types, such as astrocytes, which support motor neurons by maintaining or reinforcing internal cell protective functions, such as EAAT2 and XIAP.

Our results demonstrate pathologic improvements and retarded progression of ALS in G93A Tg rats by intrathecal administration of hrHGF from around the time of disease onset. Because HGF and c-Met are thought to be regulated in cases of not only familial but also sporadic ALS in a manner similar to the Tg mouse model of ALS (36), our findings suggest the possibility of clinical use of HGF in both familial and sporadic ALS. The results indicating the efficiency of hrHGF administration even from the onset of paralysis should prompt further clinical trials in ALS.

## ACKNOWLEDGMENT

*We thank Rieko Kamii for technical assistance.*

## REFERENCES

1. Rowland LP. Amyotrophic lateral sclerosis. *Curr Opin Neurol* 1994;7: 310–15
2. Mulder DW, Kurland LT, Offord KP, et al. Familial adult motor neuron disease: Amyotrophic lateral sclerosis. *Neurology* 1986;36:511–17

3. Rosen DR. Mutations in Cu/Zn superoxide dismutase gene are associated with familial amyotrophic lateral sclerosis. *Nature* 1993;364:362
4. Deng HX, Hentati A, Tainer JA, et al. Amyotrophic lateral sclerosis and structural defects in Cu,Zn superoxide dismutase. *Science* 1993;261:1047-51
5. Aoki M, Ogasawara M, Matsubara Y, et al. Mild ALS in Japan associated with novel SOD mutation. *Nat Genet* 1993;5:323-24
6. Kaspar BK, Llado J, Sherkat N, et al. Retrograde viral delivery of IGF-1 prolongs survival in a mouse ALS model. *Science* 2003;301:839-42
7. Azzouz M, Ralph GS, Storkebaum E, et al. VEGF delivery with retrogradely transported lentivector prolongs survival in a mouse ALS model. *Nature* 2004;429:413-17
8. Kieran D, Kalmar B, Dick JR, et al. Treatment with arimocloamol, a coinducer of heat shock proteins, delays disease progression in ALS mice. *Nat Med* 2004;10:402-5
9. Rothstein JD, Patel S, Regan MR, et al.  $\beta$ -Lactam antibiotics offer neuroprotection by increasing glutamate transporter expression. *Nature* 2005;433:73-77
10. Storkebaum E, Lambrechts D, Dewerchin M, et al. Treatment of motoneuron degeneration by intracerebroventricular delivery of VEGF in a rat model of ALS. *Nat Neurosci* 2005;8:85-92
11. Wu AS, Kiaei M, Aguirre N, et al. Iron porphyrin treatment extends survival in a transgenic animal model of amyotrophic lateral sclerosis. *J Neurochem* 2003;85:142-50
12. Crow JP, Calingasan NY, Chen J, et al. Manganese porphyrin given at symptom onset markedly extends survival of ALS mice. *Ann Neurol* 2005;58:258-65
13. Nagai M, Aoki M, Miyoshi I, et al. Rats expressing human cytosolic copper-zinc superoxide dismutase transgenes with amyotrophic lateral sclerosis: Associated mutations develop motor neuron disease. *J Neurosci* 2001;21:9246-54
14. Howland DS, Liu J, She Y, et al. Focal loss of the glutamate transporter EAAT2 in a transgenic rat model of SOD1 mutant-mediated amyotrophic lateral sclerosis (ALS). *Proc Natl Acad Sci USA* 2002;99:1604-9
15. Ochs G, Penn RD, York M, et al. A phase I/II trial of recombinant methionyl human brain derived neurotrophic factor administered by intrathecal infusion to patients with amyotrophic lateral sclerosis. *Amyotroph Lateral Scler Other Motor Neuron Disord* 2000;1:201-6
16. Ochs G, Giess R, Bendszus M, et al. Epi-arachnoidal drug deposit: A rare complication of intrathecal drug therapy. *J Pain Symptom Manage* 1999;18:229-32
17. Nakamura T, Nishizawa T, Hagiya M, et al. Molecular cloning and expression of human hepatocyte growth factor. *Nature* 1989;342:440-43
18. Jung W, Castren E, Odenthal M, et al. Expression and functional interaction of hepatocyte growth factor-scatter factor and its receptor c-met in mammalian brain. *J Cell Biol* 1994;126:485-94
19. Matsumoto K, Nakamura T. HGF: Its organotrophic role and therapeutic potential. *Ciba Found Symp* 1997;212:198-211: discussion 11-14
20. Maina F, Klein R. Hepatocyte growth factor, a versatile signal for developing neurons. *Nat Neurosci* 1999;2:213-17
21. Ebens A, Brose K, Leonardo ED, et al. Hepatocyte growth factor/scatter factor is an axonal chemoattractant and a neurotrophic factor for spinal motor neurons. *Neuron* 1996;17:1157-72
22. Sun W, Funakoshi H, Nakamura T. Overexpression of HGF retards disease progression and prolongs life span in a transgenic mouse model of ALS. *J Neurosci* 2002;22:6537-48
23. Liu KX, Kato Y, Narukawa M, et al. Importance of the liver in plasma clearance of hepatocyte growth factors in rats. *Am J Physiol* 1992;263:G642-49
24. Appasamy R, Tanabe M, Murase N, et al. Hepatocyte growth factor, blood clearance, organ uptake, and biliary excretion in normal and partially hepatectomized rats. *Lab Invest* 1993;68:270-76
25. Liu KX, Kato Y, Kino I, et al. Ligand-induced downregulation of receptor-mediated clearance of hepatocyte growth factor in rats. *Am J Physiol* 1998;275:E835-42
26. Funakoshi H, Nakamura T. Hepatocyte growth factor: From diagnosis to clinical applications. *Clin Chim Acta* 2003;327:1-23
27. Hayashi Y, Kawazoe Y, Sakamoto T, et al. Adenoviral gene transfer of hepatocyte growth factor prevents death of injured adult motoneurons after peripheral nerve avulsion. *Brain Res* 2006;1111:187-95
28. Grondard C, Biondi O, Armand AS, et al. Regular exercise prolongs survival in a type 2 spinal muscular atrophy model mouse. *J Neurosci* 2005;25:7615-22
29. Li M, Ona VO, Guegan C, et al. Functional role of caspase-1 and caspase-3 in an ALS transgenic mouse model. *Science* 2000;288:335-39
30. Friedlander RM, Brown RH, Gagliardini V, et al. Inhibition of ICE slows ALS in mice. *Nature* 1997;388:31
31. Inoue H, Tsukita K, Iwasato T, et al. The crucial role of caspase-9 in the disease progression of a transgenic ALS mouse model. *EMBO J* 2003;22:6665-74
32. Pasinelli P, Houseweart MK, Brown RH Jr. Caspase-1 and -3 are sequentially activated in motor neuron death in Cu,Zn superoxide dismutase-mediated familial amyotrophic lateral sclerosis. *Proc Natl Acad Sci USA* 2000;97:13901-6
33. Gurney ME, Pu H, Chiu AY, et al. Motor neuron degeneration in mice that express a human Cu,Zn superoxide dismutase mutation. *Science* 1994;264:1772-75
34. Gurney ME, Cutting FB, Zhai P, et al. Benefit of vitamin E, riluzole, and gabapentin in a transgenic model of familial amyotrophic lateral sclerosis. *Ann Neurol* 1996;39:147-57
35. Machide M, Hashigasako A, Matsumoto K, et al. Contact inhibition of hepatocyte growth regulated by functional association of the c-Met/hepatocyte growth factor receptor and LAR protein-tyrosine phosphatase. *J Biol Chem* 2006;281:8765-72
36. Kato S, Funakoshi H, Nakamura T, et al. Expression of hepatocyte growth factor and c-Met in the anterior horn cells of the spinal cord in the patients with amyotrophic lateral sclerosis (ALS): Immunohistochemical studies on sporadic ALS and familial ALS with superoxide dismutase 1 gene mutation. *Acta Neuropathol (Berl)* 2003;106:112-20
37. Jiang YM, Yamamoto M, Kobayashi Y, et al. Gene expression profile of spinal motor neurons in sporadic amyotrophic lateral sclerosis. *Ann Neurol* 2005;57:236-51



Review

# Regeneration-based therapies for spinal cord injuries

Hideyuki Okano<sup>a,\*</sup>, Shinjiro Kaneko<sup>a,b,c</sup>, Seiji Okada<sup>a,d</sup>, Akio Iwanami<sup>a,b,c</sup>,  
Masaya Nakamura<sup>b,\*\*</sup>, Yoshiaki Toyama<sup>b</sup>

<sup>a</sup> Department of Physiology, Keio University School of Medicine, 35 Shinanomachi, Shinjuku-ku, Tokyo 160-8582, Japan

<sup>b</sup> Department of Orthopedic Surgery, Keio University School of Medicine, Tokyo 160-8582, Japan

<sup>c</sup> Division of Neuroscience, Children's Hospital Boston, Harvard Medical School, 320 Longwood Avenue, Boston, MA 02115, USA

<sup>d</sup> SSP Stem Cell Unit, Graduate School of Medical Sciences, Kyushu University, Maidashi 3-1-1, Higashi-ku, Fukuoka 812-8582, Japan

<sup>e</sup> Clinical Research Center, National Hospital Organization, Murayama Medical Center, 2-37-1 Gakuen Musashimurayama, Tokyo 208-0011, Japan

Received 19 March 2007; received in revised form 12 April 2007; accepted 14 April 2007

Available online 1 May 2007

## Abstract

Although it has been long believed that the damaged central nervous system does not regenerate upon injury, there is an emerging hope for regeneration-based therapy of the damaged central nervous system (CNS) due to the progress of developmental biology and regenerative medicine including stem cell biology. In this review, we have summarized recent studies aimed at the development of regeneration-based therapeutic approaches for spinal cord injuries, including therapy with anti-inflammatory cytokines, transplantation of neural stem/precursor cells and induction of axonal regeneration.

© 2007 Elsevier Ltd. All rights reserved.

**Keywords:** Interleukin-6 (IL-6); Neural stem cells; Reactive astrocytes; Semaphorin 3A; Spinal cord injury (SCI); Stat3

## Contents

1. Why does the adult mammalian spinal cord lack regenerative capacities? . . . . .	68
2. Stem cells-based transplantation studies on SCI . . . . .	69
3. Supporting treatments with NSPCs-transplantation . . . . .	69
4. Insights into the regulation of cytokine signaling as a new therapy for SCI at the acute phase . . . . .	70
5. Dual roles of reactive astrocytes after SCI . . . . .	71
6. Enhancement of axonal regeneration . . . . .	71
7. Conclusion and perspectives . . . . .	72
Acknowledgements . . . . .	72
References . . . . .	72

### 1. Why does the adult mammalian spinal cord lack regenerative capacities?

Traumatic spinal cord injury (SCI) affects many people, including young people, and can result in severe damage, leading

to loss of motor and sensory function caudal to the level of injury, by severing descending and ascending fiber tracts (Ogawa et al., 2002; Okano et al., 2006). However, the effects of current conventional treatments are modest at best and consequently there is a great need for novel “regenerative” treatment strategies that could significantly protect and/or restore functions following SCI (Hofstetter, 2005). In order to develop such “regenerative” treatment strategies, it is obviously important to elucidate the underlying mechanism as to why the adult mammalian spinal cord has extremely low regenerative capacities. Many lines of evidence have indicated that apparent lack of regenerative

\* Corresponding author. Tel.: +81 3 5363 3746; fax: +81 3 3357 5445.

\*\* Corresponding author. Tel.: +81 3 5363 3812; fax: +81 3 3353 6597.

E-mail addresses: hidokano@sc.itc.keio.ac.jp (H. Okano), masa@sc.itc.keio.ac.jp (M. Nakamura).

Table 1  
Inhibitory factors for axonal regenerations and their blocking reagents

Inhibitory factors	Established molecules	Blocking reagents
Myelin-derived proteins	MAG, Nogo-A, OMgp	Nogo-66 receptor antagonist peptide (a)
Glial scar	CSPGs	C-ABC (b) Rho-kinase inhibitor (c)
Extracellular matrix-derived factors	Semaphorin3A	SM-216289 (d)

References: (a) GrandPre et al., 2002; (b) Bradbury et al., 2002; (c) Monnier et al., 2003; (d) Kaneko et al., 2006.

capacities of the adult mammalian spinal cord, could result from (i) the inhibitory character of CNS myelin and injury-induced glial scars for axonal regeneration (Table 1), (ii) the apparent inability of endogenous adult Neural Stem Cells (NSCs) in the spinal cord to induce *de novo* neurogenesis upon injury, and (iii) the lack of sufficient trophic support mechanisms (reviewed by Okano et al., 2003, 2006).

## 2. Stem cells-based transplantation studies on SCI

Experimental therapeutic methods have been previously reported on the transplantation of peripheral nerves (Richardson et al., 1980) and fetal spinal cord (Bregman, 1987) for spinal cord injuries. These studies indicated that the introduction of an appropriate environment into the injured site within the spinal cord can cause injured axons to regenerate. Practically, however, the above-mentioned protocols are almost impossible to apply for human SCI patients. For example, therapeutic approaches involving the transplantation of fetal CNS tissues came up against the double problem of obtaining a large enough amount of the donor tissues and also the ethical controversy surrounding the use of human fetal tissues.

To overcome such practical and ethical issues, transplantation therapies have been developed for SCI animal models including primates using *in vitro* expanded neural stem/precursor cells (NSPCs), including a mixed cell population of NSCs and neural precursor cells (Ogawa et al., 2002; Iwanami et al., 2005a,b; Cummings et al., 2005; Okada et al., 2005), embryonic stem (ES) cells-derived neural precursor cells (McDonald et al., 1999), or human ES cells-derived oligodendrocyte progenitor cells (OPCs). We found that appropriate time window for the *in vitro* expanded fetal NSPC transplantation is crucial to obtain the maximum therapeutic effects (Ogawa et al., 2002; Okano, 2002a,b, in press; Okano et al., 2003, 2006).

Several possible explanations for functional improvement through these transplantation studies may be advanced as follows: (1) Neurons derived from the grafted cells “relayed” signals from the disrupted fibers in the host, including local circuit interneurons or ascending fibers that existed in the dorsal column (Bregman et al., 1993); (2) oligodendrocytes derived from grafted cells might have remyelinated fibers that had been demyelinated as a result of injury and restored the salutatory conduction along the neuronal axons of long projection neuron (Cummings et al., 2005; Keirstead et al., 2005); (3) astrocytes-derived from donor neural progenitor cells might have played active roles in the generation of neuronal cells (Ogawa et al., 2002), axonal regeneration of host neuronal axons (Garcia-Abreu et al., 2000), enhancement of axonal extension of donor-derived neurons, synapse formation, and/or physiological

maturation of neuronal cells (Blondel et al., 2000); (4) trophic effects (indicating that functional improvement may not be dependent on the transplanted human fetal NSPCs, which had been expanded *in vitro*, becoming functional neurons and making the right connections, but rather on the secretion of trophic factors from the transplanted cells) might also be effective for the survival and differentiation of host cells in the injured spinal cord, leading to functional recovery. The observed functional recovery might not result from a single mechanism. On the other hand, Cummings et al. (2005) showed that engraftment of *in vitro* expanded human fetal NSPCs into the immunodeficient mouse SCI model was associated with locomotor recovery. Interestingly, observed functional recovery was abolished by selective ablation of engrafted cells by diphtheria toxin, which is selective for human cells rather than rodent cells. Thus, the survival of engrafted human fetal NSPCs, which had been expanded *in vitro*, and their progenies in the host was shown to play a role in the maintenance of improved performance. These findings indicate that differentiation of engrafted human fetal NSCs to myelinating oligodendrocytes and neurons with synaptic connections to host neurons rather than the trophic effects could be mechanisms for sustained locomotor recovery in this model.

Ogawa et al. (2002) showed that a narrow therapeutic time window can allow successful transplantation. This brief window of opportunity might arise because the microenvironment in the host spinal cord changes rapidly after the injury (Okano, 2002a,b; Okano et al., 2003). Recent reports have shown that transient severe inflammation occurs around the injured site during the acute phase, which immediately follows the injury. During this time the levels of many inflammatory cytokines that have neurotoxic or astrocyte-inducing effects, such as IL-1, IL-6, and TNF $\alpha$ , increase and then decline sharply within 24 h (Nakamura et al., 2003), indicating that the microenvironment of the acute phase is not suitable for survival of grafted cells. In fact, the transplantation of *in vitro* expanded fetal NSPCs results in mitogenic neurogenesis when the transplantation into the injured adult rat spinal cord is carried out 9 days after injury, but not when the transplantation is done within a few days of the injury (Ogawa et al., 2002). The chronic phase of spinal cord injury is not likely to be appropriate for therapeutic transplantation due to the formation of enlarged cysts and the development of glial scarring, which might inhibit axonal regeneration (reviewed by Okano, 2002a,b) (Fig. 1).

## 3. Supporting treatments with NSPCs-transplantation

To achieve greater effects of fetal or adult NSPCs-mediated cell therapy on various types of CNS damage including SCI,

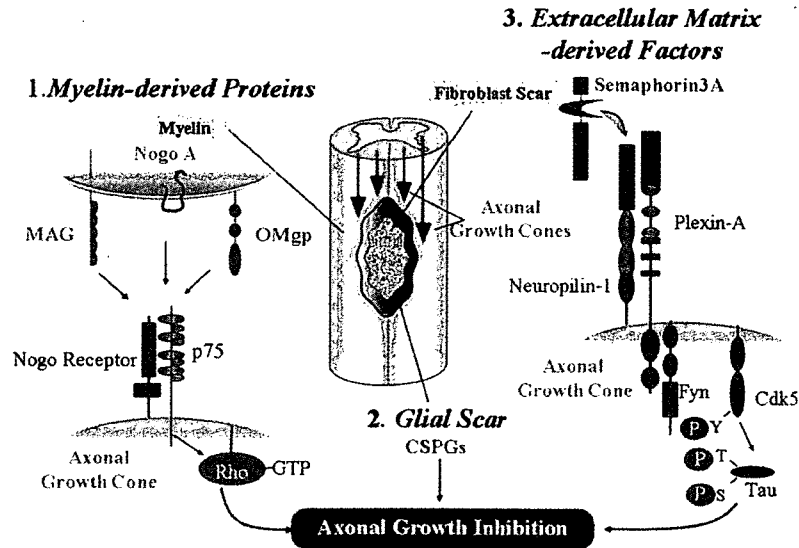


Fig. 1. Axonal growth inhibitors in the damaged CNS. Axonal growth inhibitors within the damaged CNS include (1) myelin-related proteins (e.g. MAG, NogoA and OMgp), (2) glial scar including CSPG and (3) extracellular matrix-derived factors including Semaphorin3A. Established inhibitory ligand molecules for axonal growth are marked in blue letters. These myelin-derived axonal growth cone inhibitors (MAG, NogoA and OMgp) bind to Nogo receptor expressed on the surface of the axonal growth cones and transmit inhibitory signals in axonal growth cone through p75/Rho/Rho-kinase pathways (Yamashita et al., 2002; Yamashita and Tohyama, 2003). Rho/Rho-kinase pathway is also involved in the axonal growth inhibition by glial scar-derived CSPGs (Monnier et al., 2003). Semaphorin3A, which are derived from fibroblast scar in the injured spinal cord (Kaneko et al., 2006), binds to its receptor complex including Neuropilin1/Plexin-A (Takahashi et al., 1999) and transmit its inhibitory signals through Fyn/CDK5-pathway and phosphorylation of Tau proteins (Sasaki et al., 2002).

efforts have been made to improve the therapeutic action of fetal or adult NSPCs by their genetic engineering (stem cell gene therapy) or a combination of various therapeutic interventions (e.g. scaffolds for cell therapy) together with *in vitro* expanded fetal or adult NSPCs-transplantation. For example, Lars Olson's group reported on stem cell gene therapy in a SCI model by the transduction of adult NSPCs with Neurogenin-2 (Ngn-2), a neuronal basic Helix-Loop-Helix gene. By the transplantation of Ngn-2-transduced adult NSPCs into a rat thoracic spinal cord weight-drop injury, astrocytic differentiation of engrafted cells and graft-induced sprouting and allodynia-like hypersensitivity of forepaws were shown to be suppressed (Hofstetter et al., 2005). Transduction with Ngn-2 also improved the positive effects of engrafted stem cells, including increased amounts of myelin in the injured area, recovery of hindlimb locomotor function and hindlimb sensory responses.

Although *in vitro* expanded fetal NSPC transplantation has been shown to contribute significantly to the repair of injured spinal cord in adult rats (Ogawa et al., 2002), most of the transplanted cells adhered to the cavity wall and failed to migrate and integrate into the host spinal cord in some cases. To enhance the integration of the transplanted fetal NSPCs, which had been expanded *in vitro*, we focused on chondroitin sulfate proteoglycan (CSPG) (Ikegami et al., 2005) as a putative inhibitor on NSPC migration *in vivo* that is known as a constituent of glial scar and which is strongly expressed after spinal cord injury (Fitch and Silver, 1997). Furthermore, CSPG is known to act as an inhibitor of axonal regeneration (Silver and Miller, 2004). We examined the effects of the enzymatic digestion of CSPG by chondroitinase ABC (C-ABC) upon the migration of grafted fetal NSPCs, which had been expanded *in vitro*, and axonal regeneration after SCI (Ikegami et al., 2005).

C-ABC treatment combined with *in vitro* expanded fetal NSPC transplantation into the injured spinal cord revealed that C-ABC pretreatment promoted the migration of grafted fetal NSPCs, whereas CSPG immunopositive scar tissue around the lesion cavity prevented their migration into the host spinal cord without the C-ABC pretreatment. Furthermore, these combined treatments significantly promoted the axonal regeneration at the lesion epicenter compared with the treatment using NSPC transplantation on its own (Ikegami et al., 2005). These results suggest that NSPC transplantation combined with C-ABC application may be a promising treatment strategy for regeneration of the injured spinal cord (Okano et al., 2006).

#### 4. Insights into the regulation of cytokine signaling as a new therapy for SCI at the acute phase

Insights obtained by the determining the optimal timing for transplanting fetal NSPCs gave us a hint regarding therapeutic interventions in SCI at the acute phase (Okada et al., 2004, reviewed by Okano et al., 2006). Since SCI is followed by a secondary degenerative process that includes cell death possibly due to the invasion of various inflammatory cells including macrophages and T-lymphocytes into the parenchyma of the spinal cord, it is important to prevent the secondary degenerative process by the blockade of the inflammation and invasion of inflammatory cells. Based on reports that the expression of IL-6 (Nakamura et al., 2003) and the IL-6 receptor (Okada et al., 2004) is sharply increased in the acute stages after SCI, the IL-6/IL-6 pathway could be a therapeutic target. In addition, IL-6 has also been demonstrated to play a critical role as a pro-inflammatory cytokine and to be associated with secondary tissue damage in SCI. Okada et al. (2004) assessed the efficacy of a rat anti-mouse

IL-6 receptor monoclonal antibody (MR16-1) in the treatment of acute SCI in mice. Immediately after inducing a contusion injury at the level of Th9 in mice, we administered MR16-1 by intraperitoneal injection (100 µg/g body weight). In this *in vivo* model, MR16-1-treatment decreased the number of invading inflammatory cells and the severity of connective tissue scar formation. We also found that the number of GFAP-BrdU double-positive astrocytes was suppressed by MR16-1 treatment, indicating that proliferation of astrocytes and/or mitotic production of astrocytes were inhibited by this treatment. In addition, significant functional recovery was observed in the mice treated with MR16-1 compared with control mice. These findings suggest that neutralization of IL-6 signaling in the acute phase of SCI represents an attractive option for the treatment of SCI. Humanized monoclonal antibody against human IL-6R (MRA; Atlizumab) possesses an excellent IL-6 signal inhibiting effect (Sato et al., 1993; Nishimoto et al., 2000; Choy et al., 2002). On the other hand, the biologic significance of the effects of MR16-1-treatment upon astrocytic responses still remains unclear. It is currently regarded as capable of becoming an acute phase treatment for spinal cord injury instead of high-dose steroids.

There is an increasing interest in a chemoattractant-mediated inflammatory response that is associated with secondary degeneration after SCI (Glaser et al., 2004). The chemoattractant CXCL10 is known to recruit CD4-positive T-lymphocytes via the CXCR3A receptor and inhibits angiogenesis via the CXCR3B receptor. Accordingly, Glaser et al. (2004) examined the effects of antibody-mediated functional blockade of CXCL10 upon the prevention of secondary degeneration after SCI. They found that anti-CXCL10 treatment of spinal cord injuries reduced inflammation while enhancing angiogenesis. Furthermore, they could demonstrate that anti-CXCL10 antibody treatment would support greater survival of neurons and enhance axon sprouting compared with the untreated, injured spinal cord (Glaser et al., 2006).

## 5. Dual roles of reactive astrocytes after SCI

The roles of reactive astrocytes have been controversial in the repair of damaged CNS. It was previously believed that reactive astrocytes exert detrimental roles in CNS-repair by producing barriers to inhibit axonal regeneration (Fitch and Silver, 1997; Silver and Miller, 2004). However, we recently found that reactive astrocytes also exert beneficial roles aimed at repair in the subacute phase of the injured spinal cord (Okada et al., 2006, reviewed by Okano, *in press*). At the subacute phase of SCI (from 1 to 2 weeks after SCI), astrocytes surrounding the lesion underwent a typical morphological change characteristic of 'reactive astrocytes'. These astrocytes eventually migrated centripetally to the lesion epicenter and gradually compacted the CD11b-positive inflammatory cells, contracting the lesion area up until 14 days after SCI. This could indicate the beneficial roles of reactive astrocytes. We found that the function of Stat3, which is a principal mediator in a variety of biological processes including cancer progression, wound healing and the movement of various types of cells (Hirano et al., 2000), is required for such

a migratory response in astrocytes. Reactive astrocytes in conditional Stat3 gene knockout mice (*Nestin-Cre, Stat3<sup>loxP</sup>* mice) showed limited migration and resulted in markedly widespread infiltration of inflammatory cells, neural disruption and demyelination with severe motor deficits after contusive spinal cord injury (SCI). These results suggest that Stat3 is a key regulator of reactive astrocytes in the healing process after SCI, providing a potential target for intervention in the treatment of CNS injury (Okada et al., 2006).

## 6. Enhancement of axonal regeneration

Based on the functional structure of the spinal cord, traumatic spinal cord injuries can result in severe damage, leading to loss of motor and sensory function caudal to the level of injury, by severing descending and ascending fiber tracts. Disruption of fibers that control the autonomic nervous system could lead to impairment of vascular, exocrine and endocrine gland, bowel, bladder and sexual function (Hofstetter, 2005). Accordingly, enhancement of axonal regeneration is a crucial strategy for the treatment of SCI. Several factors are shown to be involved in the inhibition of axonal regeneration after CNS trauma, such as SCI. These inhibitory factors can be classified into (1) CNS myelin-derived proteins, (2) reactive astrocytes-derived inhibitor including CSPG and (3) non-glial scar tissues-derived inhibitors, including the Semaphorine-family.

Several research groups have reported that CNS myelin-associated proteins, such as Nogo-A, MAG and OMgp play a crucial role in the inhibition of axonal regeneration (Schwab et al., 1993; Bregman et al., 1995; Chen et al., 2002; GrandPre et al., 2000; Fournier et al., 2001; Domeniconi et al., 2002; Liu et al., 2002; Olson, 2002; Wang et al., 2002a,b; Yamashita et al., 2002; Yamashita and Tohyama, 2003; Sivasankaran et al., 2004), and neutralization of Nogo-A has led to significant axonal regeneration and functional recovery after SCI (GrandPre et al., 2002). In addition to the CNS myelin-derived proteins, reactive astrocytes-derived extracellular matrix molecules, e.g. CSPGs, are also inhibitory to axonal outgrowth and manipulation of CSPGs resulted in axonal regeneration and functional recovery (Bradbury et al., 2002; Morgenstern et al., 2002). Furthermore, non-glial scar tissues-derived extracellular matrix proteins, including Semaphorin3A (Sema3A), have been reported to play major roles in the inhibition of axonal regeneration after SCI and exert an inhibitory effect on neurite extension and axonal regeneration. Recently, a small molecule agent named SM-216289, which is extracted from a fungus, was demonstrated to strongly inhibit Sema3A functions *in vitro* such as growth cone collapse and the chemorepulsive effect on neurite extension (Kikuchi et al., 2003; Kumagai et al., 2003). In order to examine the specificity of this compound, we screened various types of compounds (approximately 140,000) with a growth cone collapse assay and collagen coculture assay using embryonic day (E) 7 or 8 chick DRG, and found that this compound has a maximal inhibitory effect on Sema3A (Kaneko et al., 2006). Furthermore, we examined the pharmacological profile of SM-216289 in further detail. We obtained half-maximal inhibitory



concentration ( $IC_{50}$ ) values for receptor and ion channel binding assays, and enzyme and kinase inhibition tests. Overall, these  $IC_{50}$  values were much higher than the values for Sema3A. SM-216289 also demonstrated no agonist activity toward the receptors. We subsequently examined the effect of SM-216289 *in vivo* by administering this compound to the injured spinal cord for 4 weeks using the complete spinal cord transection model in adult rats (Kaneko et al., 2006). SM-216289-administered rats showed significantly enhanced axonal regeneration and myelination by Schwann cells, significant decreases in apoptotic cell numbers and significant enhancement of angiogenesis resulting in significantly better functional recovery. Notably, we found that SM-216289-treatment could significantly induce the regeneration of serotonergic (5-HT-positive) raphespinal tract axons that is tightly associated with locomotor functions (Bregman, 1987). Furthermore, we also found that by disrupting the 5-HT-positive raphespinal tract using the serotonin neurotoxin 5,7-dihydroxytryptamine (DHT), the functional recovery observed in the SM-216289-administered group could be substantially attenuated, suggesting that the enhanced regeneration of the 5-HT-positive raphespinal tract was at least partly responsible for the improved functional recovery observed in the SM-216289-administered group. Taken together, the current study has two major findings: first, that Sema3A contributes considerably to the inadequate axonal regeneration at the spinal cord lesion site after transection injury; and second, that SM-216289 strongly inhibits the Sema3A signal both *in vivo* and *in vitro*, and is an effective promoter of regenerative responses including axonal regeneration and/or preservation, Schwann cell-mediated myelination and axonal regeneration, angiogenesis, and the inhibition of apoptosis after spinal cord transection. These results raise the possibility of Sema3A manipulation being useful for future treatment of human SCI (Kaneko et al., 2006).

## 7. Conclusion and perspectives

As described in this review, the optimal therapeutic strategy for SCI could vary depending on the severity of the injury and time-course after the injury. We described above the blockade of the inflammatory cytokines as a treatment at the acute phase. On the other hand, we found that transplantation of *in vitro* expanded fetal NSPCs would be one of the appropriate treatments at the subacute phase after SCI. There have been a number of publications reporting the functional improvement of SCI following cell-based transplantation, including transplantation of *in vitro* expanded fetal NSPCs. However, in most of the cases, the precise underlying mechanisms for functional improvement or other benefits, which would be indispensable for development of improved therapeutic interventions for SCI patients, mostly remain to be clarified (reviewed in Steeves et al., 2004; Okano et al., 2006).

There is increasing progress on development of antagonists against inhibitors of axonal regeneration. These antagonists, including the Sema3A-inhibitor (SM-216289), have been shown to have some modest effects to induce both axonal regeneration and improvement in locomotor functions in SCI

animal models. In the future, an appropriate combination of cell-based transplantation and antagonists for inhibitors of axonal regenerations would most probably enhance their therapeutic effects for SCI.

## Acknowledgements

We are grateful to the members of the Okano Laboratory for their comments on the manuscript. This work was supported by a grant from Solution-Oriented Research for Science and Technology (SORST), Japan Science and Technology Agency (JST) and those from the Ministry of Education, Culture, Sports, Science and Technology (MEXT), Japan; the Japan Science and Technology Corporation (JST)

## References

- Bradbury, E.J., Moon, L.D.F., Popat, R.J., King, V.R., Bennett, G.S., Patel, P.N., Fawcett, J.W., McMahon, S.B., 2002. Chondroitinase ABC promotes functional recovery after spinal cord injury. *Nature* 416, 636–640.
- Bregman, B.S., 1987. Spinal cord transplants permit the growth of serotonergic axons across the site of neonatal spinal cord transection. *Dev. Brain Res.* 34, 265–279.
- Bregman, B.S., Kunkel-Bagden, E., Reier, P.J., Dai, H.N., McAtee, M., Gao, D., 1993. Recovery of function after spinal cord injury: mechanisms underlying transplant-mediated recovery of function differ after spinal cord injury in newborn and adult rats. *Exp. Neurol.* 123, 3–16.
- Bregman, B.S., Kunkel-Bagden, E., Schnell, L., 1995. Recovery from spinal cord injury mediated by antibodies to neurite growth inhibitors. *Nature* 378, 498–501.
- Blondel, O., Collin, C., McCarran, W.J., Zhu, S., Zamostiano, R., Gozes, I., Brenneman, D.E., McKay, R.D.G., 2000. A glial-derived signal regulating neuronal differentiation. *J. Neurosci.* 20, 8012–8020.
- Chen, M.S., Huber, A.B., van der Haar, M.E., Frank, M., Schnell, L., Spillmann, A.A., Christ, F., Schwab, M.E., 2002. Nogo-A is a myelin-associated neurite outgrowth inhibitor and an antigen for monoclonal antibody IN-1. *Nature* 403, 434–439.
- Choy, E.H., Isenberg, D.A., Garrood, T., Farrow, S., Ioannou, Y., Bird, H., Cheung, N., Williams, B., Hazleman, B., Price, R., Yoshizaki, K., Nishimoto, N., Kishimoto, T., Panayi, G.S., 2002. Therapeutic benefit of blocking interleukin-6 activity with an anti-interleukin-6 receptor monoclonal antibody in rheumatoid arthritis: a randomized, double-blind, placebo-controlled, dose-escalation trial. *Arthritis Rheum.* 46, 3143–3150.
- Cummings, B.J., Uchida, N., Tamaki, S.J., Salazar, D.L., Hooshmand, M., Summers, R., Gage, F.H., Anderson, A.J., 2005. Human neural stem cells differentiate and promote locomotor recovery in spinalcord-injured mice. *Proc. Natl. Acad. Sci. U.S.A.* 102, 14069–14074.
- Domeniconi, M., Cao, Z., Spencer, T., Sivasankaran, R., Wang, K.C., Nikulina, E., Kimura, N., Cai, H., Deng, K., Gao, Y., He, Z., Filbin, M.T., 2002. Myelin-associated glycoprotein interacts with the Nogo66 receptor to inhibit neurite outgrowth. *Neuron* 35, 283–290.
- Fitch, M.T., Silver, J., 1997. Glial cell extracellular matrix: boundaries for axon growth in development and regeneration. *Cell Tissue Res.* 290, 379–384.
- Fournier, A.E., GrandPre, T., Strittmatter, S.M., 2001. Identification of a receptor mediating Nogo-66 inhibition of axonal regeneration. *Nature* 409, 341–346.
- Garcia-Abreu, J., Mendes, F.A., onofre, G.R., De Freitas, M.S., Silva, L.C., Moura Neto, V., Cavalcante, L.A., 2000. Contribution of heparan sulfate to the nonpermissive role of the midline glia to the growth of midbrain neurites. *Glia* 29, 260–272.
- Glaser, J., Gonzalez, R., Perreau, V.M., Cotman, C.W., Keirstead, H.S., 2004. Neutralization of the chemokine CXCL10 enhances tissue sparing and angiogenesis following spinal cord injury. *J. Neurosci. Res.* 77, 701–708.
- Glaser, J., Gonzalez, R., Sadr, E., Keirstead, H.S., 2006. Neutralization of the chemokine CXCL10 reduces apoptosis and increases axon sprouting after spinal cord injury. *J. Neurosci. Res.* 84, 724–734.

- GrandPre, T., Nakamura, F., Vartanian, T., Strittmatter, S.M., 2000. Identification of the Nogo inhibitor of axon regeneration as a reticulon protein. *Nature* 403, 439–444.
- GrandPre, T., Li, S., Strittmatter, S.M., 2002. Nogo-66 receptor antagonist peptide promotes axonal regeneration. *Nature* 417, 547–551.
- Hirano, T., Ishihara, K., Hibi, M., 2000. Roles of STAT3 in mediating the cell growth, differentiation and survival signals relayed through the IL-6 family of cytokine receptors. *Oncogene* 19, 2548–2556.
- Hofstetter, C. 2005. Cell Therapy for Spinal Cord Injury, Studies of Motor and Sensory Systems. Thesis. Department of Neuroscience, Karolinska Institutet, Stockholm, Sweden.
- Hofstetter, C.P., Holmstrom, N.A., Lilja, J.A., Schweinhardt, P., Hao, J., Spenger, C., Wiesenfeld-Hallin, Z., Kurpad, S.N., Frisen, J., Olson, L., 2005. Allodynia limits the usefulness of intraspinal neural stem cell grafts; directed differentiation improves outcome. *Nat. Neurosci.* 8, 346–353.
- Ikegami, T., Nakamura, M., Yamane, J., Katoh, H., Okada, S., Iwanami, A., Kota, W., Ishii, K., Kato, F., Fujita, H., Takahashi, T., Toyama, Y., Okano, H., 2005. Chondroitinase ABC combined with neural stem/progenitor cell transplantation enhances their migration and axonal regeneration after rat spinal cord injury. *Eur. J. Neurosci.* 22, 3036–3046.
- Iwanami, A., Yamane, J., Katoh, H., Nakamura, M., Momomoshima, S., Ishii, H., Tanioka, Y., Tamaoki, N., Nomura, T., Toyama, Y., Okano, H., 2005a. Establishment of graded spinal cord injury model in a non-human primate: the common marmoset. *J. Neurosci. Res.* 80, 172–181.
- Iwanami, A., Kaneko, S., Nakamura, M., Kanemura, Y., Mori, H., Kobayashi, S., Yamasaki, M., Momomoshima, S., Ishii, H., Ando, K., Tanioka, Y., Tamaoki, N., Nomura, T., Toyama, Y., Okano, H., 2005b. Transplantation of human neural stem/progenitor cells promotes functional recovery after spinal cord injury in common marmoset. *J. Neurosci. Res.* 80, 182–190.
- Kaneko, S., Iwanami, A., Nakamura, M., Kishino, A., Kikuchi, K., Shibata, S., Okano, H.J., Ikegami, T., Moriya, A., Konishi, O., Nakayama, C., Kumagai, K., Kimura, T., Sato, Y., Goshima, Y., Taniguchi, M., Ito, M., He, Z., Toyama, Y., Okano, H., 2006. A selective Sema3A-inhibitor enhances regenerative responses and functional recovery of the injured spinal cord. *Nat. Med.* 12, 1380–1389.
- Keirstead, H.S., Nistor, G., Bernal, G., Totoiu, M., Cloutier, F., Sharp, K., Steward, O., 2005. Human embryonic stem cell-derived oligodendrocyte progenitor cell transplants remyelinate and restore locomotion after spinal cord injury. *J. Neurosci.* 25, 4694–4705.
- Kikuchi, K., Kishino, A., Konishi, O., Kumagai, K., Hosotani, N., Saji, I., Nakayama, C., Kimura, T., 2003. In vitro and in vivo characterization of a novel Semaphorin 3A inhibitor, SM-216289 or xanthofulvin. *J. Biol. Chem.* 278, 42985–42991.
- Kumagai, K., Hosotani, N., Kikuchi, K., Kimura, T., Saji, I., 2003. Xanthofulvin, a novel semaphorin inhibitor produced by a strain of *Penicillium*. *J. Antibiot.* 56, 610–616.
- Liu, B.P., Fournier, A., GrandPre, T., Strittmatter, S.M., 2002. Myelin-associated glycoprotein as a functional ligand for the Nogo-66 receptor. *Science* 297, 1190–1193.
- McDonald, J.W., Liu, X.Z., Qu, Y., Liu, S., Mickey, S.K., Turetsky, D., Gottlieb, D.I., Choi, D.W., 1999. Transplanted embryonic stem cells survive, differentiate and promote recovery in injured rat spinal cord. *Nat. Med.* 5, 1410–1412.
- Monnier, P.P., Sierra, A., Schwab, J.M., Henke-Fahle, S., Mueller, B.K., 2003. The Rho/ROCK pathway mediates neurite growth-inhibitory activity associated with the chondroitin sulfate proteoglycans of the CNS glial scar. *Mol. Cell Neurosci.* 22, 319–330.
- Morgenstern, D.A., Asher, R.A., Fawcett, J.W., 2002. Chondroitin sulphate proteoglycans in the CNS injury response. *Prog. Brain Res.* 137, 313–332.
- Nakamura, M., Houghtling, R.A., MacArthur, L., Bayer, B.M., Bregman, B.S., 2003. Differences in cytokine gene expression profile between acute and secondary injury in adult rat spinal cord. *Exp. Neurol.* 184, 313–325.
- Nishimoto, N., Sasai, M., Shima, Y., Nakagawa, M., Matsumoto, T., Shirai, T., Kishimoto, T., Yoshizaki, K., 2000. Improvement in Castleman's disease by humanized anti-interleukin-6 receptor antibody therapy. *Blood* 95, 56–61.
- Ogawa, Y., Sawamoto, K., Miyata, T., Miyao, S., Watanabe, M., Toyama, Y., Nakamura, M., Bregman, B.S., Koike, M., Uchiyama, Y., Toyama, Y., Okano, H., 2002. Transplantation of in vitro expanded fetal neural progenitor cells results in neurogenesis and functional recovery after spinal cord contusion injury in rats. *J. Neurosci. Res.* 69, 925–933.
- Okada, S., Nakamura, M., Mikami, Y., Shimazaki, T., Mihara, M., Ohsugi, Y., Iwamoto, Y., Yoshizaki, K., Kishimoto, T., Toyama, Y., Okano, H., 2004. Blockade of interleukin-6 receptor suppresses reactive astrogliosis and ameliorates functional recovery in experimental spinal cord injury. *J. Neurosci. Res.* 76, 265–276.
- Okada, S., Ishii, K., Yamane, J., Iwanami, A., Ikegami, T., Iwamoto, Y., Nakamura, M., Miyoshi, H., Okano, H.J., Contag, C.H., Toyama, Y., Okano, H., 2005. In vivo imaging of engrafted neural stem cells: its application in evaluating the optimal timing of transplantation for spinal cord injury. *FASEB J.* 19, 1839–1841.
- Okada, S., Ishii, K., Miyao, T., Shimazaki, T., Katoh, H., Yamane, J., Yoshimura, A., Iwamoto, Y., Nakamura, M., Toyama, Y., Okano, H., 2006. Conditional ablation of STAT3/SOCS3 discloses a dual role for reactive astrocytes after spinal cord injury. *Nat. Med.* 12, 829–834.
- Okano, H., 2002a. The stem cell biology of the central nervous system. *J. Neurosci. Res.* 69, 698–707.
- Okano, H., 2002b. Neural stem cells: progression of basic research and perspective for clinical application. *Keio J. Med.* 51, 115–128.
- Okano, H., Ogawa, Y., Nakamura, M., Kaneko, S., Iwanami, A., Toyama, A., 2003. Transplantation of neural stem cells into the spinal cord after injury. *Semin. Cell Dev. Biol.* 14, 191–198.
- Okano, H., Nakamura, M., Toyama, Y., 2006. Stem cell therapies for injured spinal cord. *Inflamm. Regen.* 26, 18–28.
- Okano H., in press. Transplantation of neural stem cells for spinal cord regeneration. In: Binder, D., Hirokawa, N., Windhorst, U. (Eds.), *Encyclopedic References of Neuroscience*. Springer-Verlag, Heidelberg, Germany.
- Olson, L., 2002. Medicine: clearing a path for nerve growth. *Nature* 416, 589–590.
- Richardson, P.M., McGuinness, U.M., Aguayo, A.J., 1980. Axons from CNS neurons regenerate into PNS grafts. *Nature* 284, 264–265.
- Sasaki, Y., Cheng, C., Uchida, Y., Nakajima, O., Ohshima, T., Yagi, T., Taniguchi, M., Nakayama, T., Kishida, R., Kudo, Y., Ohno, S., Nakamura, F., Goshima, Y., 2002. Fyn and Cdk5 mediate semaphorin-3A signaling which is involved in regulation of dendrite orientation in cerebral cortex. *Neuron* 35, 907–920.
- Sato, K., Tsuchiya, M., Saldanha, J., Koishihara, Y., Ohsugi, Y., Kishimoto, T., Bendig, M.M., 1993. Reshaping a human antibody to inhibit the interleukin 6-dependent tumor cell growth. *Cancer Res.* 53, 851–856.
- Schwab, M.E., Kapfhammer, J.P., Bandtlow, C.E., 1993. Inhibitors of neurite growth. *Annu. Rev. Neurosci.* 16, 565–595.
- Sivasankaran, R., Pei, J., Wang, K.C., Zhang, Y.P., Shields, C.B., Xu, X.M., He, Z., 2004. PKC mediates inhibitory effects of myelin and chondroitin sulfate proteoglycans on axonal regeneration. *Nat. Neurosci.* 7, 261–268.
- Silver, J., Miller, J.H., 2004. Regeneration beyond the glial scar. *Nat. Rev. Neurosci.* 5, 146–156.
- Steeves, J., Fawcett, J., Tuszynski, M., 2004. Report of international clinical trials workshop on spinal cord injury, February 20–21, 2004, Vancouver, Canada. *Spinal Cord.* 42, 591–597.
- Takahashi, T., Fournier, A., Nakamura, F., Wang, L.H., Murakami, Y., Kalb, R.G., Fujisawa, H., Strittmatter, S.M., 1999. Plexin-neuropilin-1 complexes form functional semaphorin-3A receptors. *Cell* 99, 59–69.
- Wang, K.C., Koprivica, V., Kim, J.A., Sivasankaran, R., Guo, Y., Neve, R.L., He, Z., 2002a. Oligodendrocyte-myelin glycoprotein is a Nogo receptor ligand that inhibits neurite outgrowth. *Nature* 417, 941–944.
- Wang, K.C., Kim, J.A., Sivasankaran, R., Segal, R., He, Z., 2002b. p75 interacts with the Nogo receptor as a co-receptor for Nogo, MAG and OMgp. *Nature* 420, 74–78.
- Yamashita, T., Higuchi, H., Tohyama, M., 2002. The p75 receptor transduces the signal from myelin-associated glycoprotein to Rho. *J. Cell. Biol.* 157, 565–570.
- Yamashita, T., Tohyama, M., 2003. The p75 receptor acts as a displacement factor that releases Rho from Rho-GDI. *Nat. Neurosci.* 6, 461–467.

# Hepatocyte Growth Factor Promotes Endogenous Repair and Functional Recovery After Spinal Cord Injury

Kazuya Kitamura,<sup>1,2</sup> Akio Iwanami,<sup>1–3</sup> Masaya Nakamura,<sup>1</sup> Junichi Yamane,<sup>1,2</sup> Kota Watanabe,<sup>1</sup> Yoshinori Suzuki,<sup>4</sup> Daisuke Miyazawa,<sup>4</sup> Shinsuke Shibata,<sup>2</sup> Hiroshi Funakoshi,<sup>4</sup> Shinichi Miyatake,<sup>5</sup> Robert S. Coffin,<sup>6</sup> Toshikazu Nakamura,<sup>4</sup> Yoshiaki Toyama,<sup>1</sup> and Hideyuki Okano<sup>2\*</sup>

<sup>1</sup>Department of Orthopaedic Surgery, Keio University School of Medicine, Shinjuku, Tokyo, Japan

<sup>2</sup>Department of Physiology, Keio University School of Medicine, Shinjuku, Tokyo, Japan

<sup>3</sup>Clinical Research Center, National Hospital Organization, Murayama Medical Center, Musashimurayama, Tokyo, Japan

<sup>4</sup>Division of Molecular Regenerative Medicine, Osaka University Graduate School of Medicine, Suita, Osaka, Japan

<sup>5</sup>Department of Neurosurgery, Osaka Medical College, Takatsuki, Osaka, Japan

<sup>6</sup>Department of Molecular Pathology, Windeyer Institute of Medical Science of University College, London, United Kingdom

Many therapeutic interventions using neurotrophic factors or pharmacological agents have focused on secondary degeneration after spinal cord injury (SCI) to reduce damaged areas and promote axonal regeneration and functional recovery. Hepatocyte growth factor (HGF), which was identified as a potent mitogen for mature hepatocytes and a mediator of inflammatory responses to tissue injury, has recently been highlighted as a potent neurotrophic and angiogenic factor in the central nervous system (CNS). In the present study, we revealed that the extent of endogenous HGF up-regulation was less than that of c-Met, an HGF receptor, during the acute phase of SCI and administered exogenous HGF into injured spinal cord using a replication-incompetent herpes simplex virus-1 (HSV-1) vector to determine whether HGF exerts beneficial effects and promotes functional recovery after SCI. This treatment resulted in the significant promotion of neuron and oligodendrocyte survival, angiogenesis, axonal regrowth, and functional recovery after SCI. These results suggest that HGF gene delivery to the injured spinal cord exerts multiple beneficial effects and enhances endogenous repair after SCI. This is the first study to demonstrate the efficacy of HGF for SCI. © 2007 Wiley-Liss, Inc.

**Key words:** hepatocyte growth factor; spinal cord injury; repair; functional recovery

Spinal cord injury (SCI) is followed by secondary degeneration, which is characterized by progressive tissue necrosis, and many experimental interventions using neurotrophic factors have focused on this posttraumatic inflammatory process to reduce damaged area and promote axonal regeneration throughout the lesion epicen-

ter. Neurotrophins such as nerve growth factor (NGF; Tuszynski et al., 1994, 1996), brain-derived growth factor (BDNF; Jakeman et al., 1998; Vavrek et al., 2006), neurotrophin-3 (NT-3; Grill et al., 1997; McTigue et al., 1998), and glial cell line-derived neurotrophic factor (GDNF; Liu et al., 1999; Blesch and Tuszynski, 2001) have been reported to enhance axonal growth in injured spinal cord, and some of the studies cited above showed that neurotrophins promoted behavioral recovery after SCI (Jakeman et al., 1998; Liu et al., 1999).

Not only neurotrophic support but also angiogenesis after SCI is a critical factor in the endogenous regenerative response to trauma (Casella et al., 2002; Loy et al., 2002). Initial damage to local blood vessels is decisive for the progression of destructive events during secondary degeneration (Mautes et al., 2000) and strategic treatments to improve angiogenesis after SCI showed a relationship between blood flow and functional recovery (Glaser et al., 2004; Guizar-Sahagun et al., 2005). Hepatocyte growth

The first two authors contributed equally to this work.

Contract grant sponsor: Leading Project for the Realization of Regenerative Medicine from the Ministry of Education, Culture, Sports, Science and Technology (MEXT), Japan; Contract grant sponsor: General Insurance Association of Japan; Contract grant sponsor: Terumo Foundation Life Science Foundation (to H.O.); Contract grant sponsor: Grant-in-Aid for the 21st Century COE Program from MEXT (to Keio University); Contract grant sponsor: Keio Gijuku Academic Development Funds.

\*Correspondence to: Hideyuki Okano, 35 Shinanomachi, Shinjuku-ku, Tokyo 160-8582, Japan. E-mail: hidokano@sc.itc.keio.ac.jp

Received 1 March 2007; Accepted 26 March 2007

Published online 4 June 2007 in Wiley InterScience (www.interscience.wiley.com). DOI: 10.1002/jnr.21372

factor (HGF) was first identified as a potent mitogen for mature hepatocytes (Nakamura et al., 1984; Nakamura et al., 1989) and a natural ligand for the c-Met protooncogene product (Bottaro et al., 1991). Recent studies have revealed that HGF acts as a neurotrophic factor in a variety of neurons (Hamanoue et al., 1996; Maina and Klein, 1999; Caton et al., 2000) and that HGF administration enhances angiogenesis, improves microcirculation, inhibits the destruction of the blood-brain barrier (Date et al., 2004), and exerts a neuroprotective effects after cerebral ischemia (Miyazawa et al., 1998; Shimamura et al., 2006). In the present study, we first examined the changes in endogenous HGF and c-Met expression after rat SCI and then determined whether the administration of exogenous HGF into the injured spinal cord using HSV-1 vector had positive effects on histological changes and the motor function after SCI. To the best of our knowledge, this is the first study to examine the efficacy of HGF for SCI.

## MATERIALS AND METHODS

### Administration of HGF by HSV-1 Vector and SCI

Adult female Sprague-Dawley rats (230–250 g; Clea, Tokyo, Japan) were used for all the experimental groups. All animals were handled in accordance with the Laboratory Animal Welfare Act, the *Guide for the care and use of laboratory animals* (National Institutes of Health), and the guidelines and policies for animal surgery provided by the Animal Study Committee of the Central Institute for Experimental Animals of Keio University. Rreplication-incompetent HSV-1 vectors, HSV-HGF and HSV-LacZ, were obtained as described by Zhao et al. (2006). Rats were anesthetized, their spinal cords were exposed by laminectomy at T10, and 10  $\mu$ l of HSV-HGF or HSV-LacZ (each titer  $1.3 \times 10^9$  pfu/ml) was injected into the spinal cord in the HGF group or the LacZ group, respectively ( $n = 62$  each). At 3 days after HSV-1 vector injection, the spinal cords were again exposed at the site of injection, and the region was contused by using the Infinite Horizon impactor (200 kdyn; Precision Systems, Lexington, KY). In the SCI group, contusive SCI was induced at T10 using the IH impactor without the prior injection of HSV-1 vectors ( $n = 75$ ).

### Enzyme-Linked Immunosorbent Assay

Plasma samples were withdrawn transcardially, and a 4-mm-long segment of spinal cord at T10 was isolated and lysed at the indicated times. The spinal cord lysates were prepared with 50 mM Tris-HCl (pH 7.4), 2 M NaCl, 25 mM  $\beta$ -glycerophosphate, 25 mM NaF, 1% Triton X-100, 1 mM phenylmethylsulfonylfluoride (PMSF; Wako, Osaka, Japan), 2 mg/ml antipain (Peptide Institute Inc., Osaka, Japan), 2 mg/ml leupeptin (Peptide Institute Inc.), and 2 mg/ml pepstatin (Peptide Institute Inc.). The concentrations of HGF protein in the extracts of spinal cords lysates and plasma were determined by using ELISA kits (Institute of Immunology, Tokyo, Japan).

### Real-Time Quantitative RT-PCR

A 4-mm-long spinal cord segment at T10 was collected at indicated times, and total RNA was isolated from each spinal cord sample using an RNeasy Kit (Qiagen, Bethesda,

MD). The levels of HGF and c-Met mRNA were measured as previously described (Sun et al., 2000). The quantitative data for each sample at indicated times was used to determine the ratio relative to that in intact spinal cord.

### Immunoblotting Analysis

Lysates from each 4-mm-long spinal cord at T10 were prepared in the same buffer used in an ELISA at indicated times. Proteins (20  $\mu$ g) were resolved via SDS-PAGE, transferred to a polyvinylidene difluoride membrane, and immunoblotted with a polyclonal antibody (anticleaved caspase-3; 1:500; Cell Signaling Technology, Beverly, MA). Bands were visualized by using an ECL Blotting Analysis System (Amersham Bioscience, Arlington Heights, IL), and the band intensities were measured with an NIH image analyzer. The quantitative data for each band show the relative ratio to that of the spinal cord lysate at 3 days after SCI without any HSV-1 vector injection.

### Immunohistochemistry

Spinal cords were perfusion fixed with 4% paraformaldehyde in 0.1 M phosphate-buffered saline (PBS) and postfixed in the same fixative (24 hr), 10% sucrose in 0.1 M PBS (24 hr), and 30% sucrose in 0.1 M PBS (24 hr). Segments of spinal cords were embedded in optimal cutting temperature compound and cut on a cryostat into 20- $\mu$ m-thick sections. For immunofluorescence staining, the sections were incubated at 4°C with monoclonal anti-NeuN (1:200; Chemicon, Temecula, CA), monoclonal antigial fibrillary acidic protein (GFAP; 1:500; Sigma, St. Louis, MO), monoclonal anti-GST- $\pi$  (1:500; BD Bioscience Pharmingen, San Diego, CA), and polyclonal anti-c-Met (1:50; Santa Cruz Biotechnology, Santa Cruz, CA), followed by Alexa Fluoro-conjugated secondary antibodies (1:500; Molecular Probes, Eugene, OR) and polyclonal anti-rat HGF (1:1; Institute of Immunology) and polyclonal anticleaved caspase-3 (1:400; Cell Signaling), followed by biotinylated secondary antibodies (1:500; Jackson Immunoresearch, West Grove, PA). For diaminobenzidine staining, the sections were incubated at 4°C with polyclonal anti-5-hydroxytryptamine (5-HT; 1:100; Dia Sorin, Stillwater, MN), polyclonal anticholine acetyltransferase (ChAT; 1:50; Chemicon), monoclonal anti-rat endothelial cell antigen-1 (RECA-1; 1:25; Serotec, Raleigh, NC), monoclonal anti-growth-associated protein-43 (GAP-43; 1:2,000; Chemicon), and monoclonal antineurofilament 200 kD (RT97; 1:2,000; Chemicon), followed by biotinylated secondary antibodies (1:500; Jackson Immunoresearch). Biotinylated antibodies were visualized using the Vectastain Elite ABC kit (Vector Laboratories, Burlingame, CA), followed by TSA (Vector Laboratories) or diaminobenzidine (Sigma). All the images were obtained via microscopy (Axioskop 2 Plus; Zeiss, Oberkochen, Germany) or confocal microscopy (LSM510; Zeiss).

### Quantitative Analyses

To quantify the RECA-1-positive area and Luxol fast blue (LFB)-stained myelinated area, the images of axial sections were obtained. To quantify the area of the GAP-43-positive fibers and the RT97-positive fibers, the midsagittal sections were scanned and tiled transversely throughout a cephalocaudal